

Thermodynamics of Optical Cooling of Bulk Matter

Carl E. Mungan

Physics Department, United States Naval Academy

Annapolis, MD 21402-5002

I. Introduction

It initially seems surprising that one can optically cool bulk material, be it a condensed sample or a gas of more than the comparatively low number of atoms used in Doppler cooling experiments (Wineland and Itano 1987). Part of the surprise arises from the novelty and is dispelled when one understands that the thermal energy withdrawn from the material is carried away by the radiation emitted by it (and presumably absorbed at some external heat sink that is not in thermal contact with the sample). But this explanation in terms of the first law of thermodynamics (that is, of the balance between the cooling rate and the net optical power output from the refrigerating sample) is not fully satisfying. Further thought still leaves one perplexed, as it appears that “heat” is being converted into light whose spectrum is clearly narrower than that of Planckian thermal radiation, suggesting that entropy is being reduced in violation of the second law of thermodynamics. What is missing from the analysis is an accounting of the entropy of the pump source. The reason one uses a laser to pump the refrigerator (in the case of a photoluminescent cooler) or a current source (for an electroluminescent cooler) is that it is a low-entropy input of energy; ideally a laser beam or electric current is analogous to the “work” used to drive a refrigerator. One can therefore summarize the input and output sources of energy to and from an optical refrigerator by the schematic diagram in Fig. 1. The principal goal of the present chapter is to quantify these energy and entropy fluxes in order to characterize the refrigeration potential.

The overall organization is as follows. By way of background, Sec. II presents a selected review of the history and literature of the thermodynamics of fluorescent cooling of bulk matter. Next, Sec. III describes how one relates the entropy to the energy carried by an optical beam and defines various radiation temperatures; specific examples are included to make the formulae concrete. Then Sec. IV uses those results to calculate the Carnot coefficient of performance of typical solid-state coolers for which actual operating efficiencies have been measured experimentally; various corrections for real-world inefficiencies are also quantified. In Sec. V, some key ideas are summarized and the thermodynamics of a few topics related to optical refrigeration are briefly discussed, notably radiation-balanced lasing and the recycling of output optical energy back to the input.

II. Historical Review of Optical Cooling Thermodynamics

In a German paper written over three quarters of a century ago, Peter Pringsheim (1929) argued that net cooling of a sodium vapor by resonant anti-Stokes emission would not violate the second law of thermodynamics, in contrast to a blanket assertion to the contrary made by Lenard, Schmidt, and Tomaschek. Pringsheim proposed that Na vapor in a glass cell will emit on both yellow D lines when only the lower frequency D_1 transition is pumped, as sketched in Fig. 2. Define the fluorescence quantum efficiency η to be the ratio of the number of emitted to absorbed photons (averaged over a long interval compared to the relaxation time τ) and assume it is equal to unity for a sodium vapor at low enough pressure that collisional de-excitations from the upper P to the lower S levels can be neglected. Noting that the average output photon energy is larger than that of the input, one then concludes that the vapor will cool down (until a balance with the heat leak from the surroundings is achieved).

Pringsheim suggested that this optical cooling process can be reconciled with the second law by noting that the sodium vapor is not a closed system—energy is being input in the form of pump light to drive the cooling cycle. But sixteen years later, Vavilov (1945) at the Academy of Sciences in Moscow objected that the system is also outputting light, and more radiative energy is leaving it than is entering. Suppose, he argued, that we were to convert the emitted light into electrical energy (using an optical piston for example) and use that to drive the pump lamp. In that case, it would appear that one could build a self-contained system (lamp, vapor sample, and photovoltaic converter) that transforms thermal energy into useful work in the form of the small excess electrical energy converted. He further pointed out that available experimental data for the fluorescence spectra of organic dyes indicated that the quantum yield ρ (defined as the ratio of the average fluorescence frequency ν_F to the pump frequency ν_P) was always less than unity.

Pringsheim (1946) replied by noting that the entropy of the emitted radiation is larger than that of the absorbed radiation because the pump light is monochromatic and unidirectional while the fluorescence is broadband and isotropic. One might colloquially say that the latter light waves are more “disordered” (both spectrally and spatially) than the former. (Nowadays, using laser sources, one might add phase coherence to the list of differences between the pump and fluorescence radiation.) Spontaneous luminescence is an intrinsically irreversible process, and so a reversible cooling cycle whose sole effect is the “conversion of heat into work” is not possible. Pringsheim also argued that anti-Stokes fluorescence from dye solutions due to emission between different vibrational levels of two electronic bands can in principle occur with a quantum yield greater than one. If this is not seen in actual experiments, that could be because the fluorescence quantum efficiency is less than one and it might even be frequency dependent, if

molecules in the spectral wings are subject to greater perturbations by the solvent than those near the line center.

On the journal pages immediately following Pringsheim's reply are two papers by Vavilov (1946) and Landau (1946). In the former, Vavilov makes two new arguments. First, he asserts that the loss of directionality of the fluorescence cannot be associated with an increase in entropy because one can surround the sample with a set of collimating lenses and plane mirrors to steer every emitted ray into essentially the same direction. While true, this argument is nevertheless irrelevant because the entropy of radiation (introduced quantitatively in Landau's paper) is actually an integral over the product of a beam's cross-sectional area and solid-angle divergence (and not over the latter alone) and by Liouville's theorem that brightness product cannot be decreased by a passive collection of lenses and mirrors (Arakengy 1957). Second, Vavilov noted the conflicting requirements of making the pressure of the sodium gas low enough to obviate nonradiative relaxation from the P down to the S levels, while keeping the pressure high enough to ensure thermal equilibration between the two excited P levels. Since both processes are mediated by atomic collisions, it is clear that one cannot simultaneously satisfy these two requirements perfectly. While admitting Vavilov's point, it nonetheless cannot be concluded that fluorescent cooling of a gas is infeasible—as a counter-example, modern experiments have demonstrated anti-Stokes cooling of carbon dioxide (Djeu and Whitney 1981; Liakhou *et al.* 2004). In retrospect, one can argue that the energy exchanged between two colliding atoms can at most be of order $kT = 25$ meV at room temperature (where k is Boltzmann's constant). This estimate implies that a single collision can readily transfer atoms from either excited P level to the other. In contrast, the energy gap between these excited levels and the ground S state is about $80kT$, which means that de-excitation by collisions between sodium atoms is strongly suppressed. (On the other hand, collisional relaxation at the walls of the gas cell is much more likely because of the large effective spring constant of the matrix-bonded glass atoms. In fact, in the carbon dioxide experiments mentioned above, cooling only occurs along the central axis of the long cylindrical cell, well away from its curved surface.) The point is that there is a definite crossover region in the gas density: high enough that the rate of collisions between pairs of atoms is large compared to the radiative relaxation rate $1/\tau_R$ but low enough that simultaneous collisions between many atoms seldom occur.

Interestingly enough, if we assume that the cooling coefficient of performance κ is roughly equal to the standard Carnot value for a refrigerator,

$$\kappa_C = \frac{T_L}{T_H - T_L} \tag{1}$$

where the low-temperature reservoir is taken to be the optical cooler operating near room temperature, $T_L = 300 \text{ K}$, and the hot reservoir is taken to be the “effective temperature” (whose meaning is clarified below) of the waste fluorescence, with T_H estimated by Landau (1946) to be say $10\,000 \text{ K}$, then one finds $\kappa \approx 3\%$. This is remarkably close to the measured values of the best currently known optical coolers, as recently reviewed by Mungan *et al.* (2007). Therefore despite Vavilov’s objections, one can reasonably assert that the basic theoretical validity of the concept of optical cooling of bulk matter was already established in his era. However, practical implementations of the idea, pioneered by the experiments of Kushida and Geusic (1968) using $\text{Nd}^{3+}:\text{YAG}$, had to await the invention of the laser.

A more accurate expression for the Carnot coefficient of performance (COP) than Eq. (1) follows from the work of Geusic, Schulz-DuBois, and Scovil (1967). They point out that there are actually three temperatures (not just two) to be considered: the temperature of the cooling sample T , the effective temperature of the fluorescence T_F , and the effective temperature of the pump T_P . As above, we assume that T_F is substantially larger than T . In addition, since the pump radiation must have much lower entropy flux than the fluorescence (in order to satisfy the second law of thermodynamics) with approximately the same power, it follows that $T_P \gg T_F$. One can therefore schematize the situation with three thermal reservoirs arranged in vertically decreasing order of temperature as in Fig. 3. A refrigerator operates between the lower two reservoirs, with a Carnot COP of

$$\kappa_{\text{fridge,C}} = \frac{T}{T_F - T} \quad (2)$$

by substituting the appropriate high and low temperatures into Eq. (1). The work W required to drive the operation of this fridge comes from a heat engine operating between the upper two reservoirs. The usual expression for its Carnot efficiency is

$$\varepsilon_{\text{engine,C}} = \frac{T_P - T_F}{T_P} \quad (3)$$

By multiplying together Eqs. (2) and (3), we obtain the overall Carnot coefficient of performance of the optical cooler,

$$\kappa_C = \frac{T - \Delta T}{T_F - T} \quad (4)$$

where $\Delta T \equiv T T_F / T_P$ represents a correction to the temperature in the numerator, slightly decreasing the COP than what it otherwise would have been. An analogous expression can be deduced for the Carnot efficiency of an optically pumped laser, which is essentially an optical cooler running in reverse (Landsberg and Evans 1968; Kafri and Levine 1974; Mungan 2005).

Note that $T_p \rightarrow \infty$ for an ideal laser or electric-current pump source, in which case Eq. (4) reduces to

$$\kappa_C = \frac{T}{T_F - T}, \quad (5)$$

in agreement with the preceding discussion of Eq. (1). This Carnot COP falls approximately linearly to zero as $T \rightarrow 0$ starting from a sample temperature substantially below T_F .

Now consider coupling these temperature baths to a nondegenerate three-level system like that of Fig. 2, resulting in the arrangement sketched in Fig. 4. Let the population densities in the three levels be N_1 , N_2 , and N_3 . Since levels 2 and 3 thermalize with the sample, their population ratio follows a Boltzmann distribution,

$$\frac{N_3}{N_2} = e^{-h\nu_{23}/kT} \quad (6)$$

where h is Planck's constant and where the transition frequency between levels 2 and 3 is the difference between the emission and excitation frequencies, $\nu_{23} = \nu_F - \nu_P$. Let us similarly assume that the pump source consists of a spectrally filtered arc discharge lamp that is coupled to the system in such a fashion that we get a Boltzmann population ratio between levels 1 and 2 determined by the thousands of degrees temperature T_p of the arc,

$$\frac{N_2}{N_1} = e^{-h\nu_P/kT_p}. \quad (7)$$

Multiplying Eqs. (6) and (7) together and setting the result equal to

$$\frac{N_3}{N_1} = e^{-h\nu_F/kT_F} \quad (8)$$

defines an effective temperature of the fluorescence, $T_F = T T_p \nu_F / (T_p \nu_F - T_p \nu_P + T \nu_P)$. Substituting this result into Eq. (4) in the form $\kappa_C = (1 - T_F / T_p) / (T_F / T - 1)$ gives rise to

$$\kappa_C = \frac{\nu_F - \nu_P}{\nu_P} = \frac{\lambda_P - \lambda_F}{\lambda_F} \quad (9)$$

where in the second equality the pump and mean fluorescence vacuum wavelengths are the speed of light c divided by the corresponding frequencies. Note that the first equality accords with the definition of the COP as Q / E_{in} , the ratio of the net cooling energy to the (absorbed) pump energy per cycle, so that Figs. 3 and 4 are consistent with each other. (One can also express this equality as $\kappa_C = \rho - 1$ in terms of the quantum yield discussed above.) This result assumes that the heat engine and refrigerator in Fig. 3 are ideal devices, so that entropy is conserved. In practice, however, fluorescence is a spontaneous (irreversible) process and the energy transfers

to and from the thermal reservoirs do not proceed quasistatically, which means the actual coefficient of performance cannot attain the Carnot value given by Eq. (4).

To numerically estimate this ideal cooling efficiency, we can approximate the difference between the emission and excitation photon energies in Fig. 4 by a thermally absorbed energy of kT . In that case, Eq. (9) becomes $\kappa_C \approx kT\lambda_p / hc$ which at room temperature is equal to 2% for 1- μm excitation. This value is in good agreement with experimental measurements on the laser cooling of ytterbium doped in a heavy-metal-fluoride glass (Epstein *et al.* 1995).

Landau (1946) defined the effective temperature T_F of the fluorescence by what is nowadays called its “brightness temperature,” which is the temperature of a blackbody whose spectral radiance is equal to that of the fluorescence averaged over its bandwidth (assumed to be narrow). This is also the radiation temperature used by Ross (1966), but he distinguished it in general from temperature T_H owing to energy losses. Weinstein (1960) appears to have been the first person to define the effective temperature instead in terms of a second, distinct quantity that has been dubbed the “flux temperature” by Landsberg and Tonge (1980). The flux temperature is the ratio of the energy and entropy carried by a beam of light. (Careful mathematical definitions of the brightness and flux temperatures appear in Sec. III below.) Weinstein used Eq. (5) to compute the maximum visible emission efficiency, $1 + \kappa_C$, of an electrically pumped lamp or phosphor.

A more logical choice of electroluminescent cooler than a lamp or phosphor is a semiconductor diode. It was noted in the early 1950s that the threshold voltage for recombination emission across a p - n junction in silicon carbide is slightly smaller than its bandgap, which could therefore lead to a cooling effect (Lehovec *et al.* 1953). In brief follow-up papers, Tauc (1957) and Gerthsen and Kauer (1965) argued that the idealized cooling COP is

$$\kappa = \frac{E_g - eV}{eV} \quad (10)$$

where E_g is the bandgap energy, e is the electron charge, and V is the forward bias voltage. This expression assumes unit external fluorescence quantum efficiency and zero Joule heating. If we identify the mean emission frequency as $\nu_F = E_g / h$ and the pump energy as $h\nu_P = eV$ per electron, then Eq. (10) is seen to be the direct analog of Eq. (9). But it is more accurate to obtain ν_F from an actual measurement of the emission spectrum (rather than assuming it is equal to the bandgap frequency), in which case we can rewrite Eq. (10) as

$$\kappa = \frac{h\nu_F}{eV} - 1. \quad (11)$$

For example, if one estimates ν_F to be the near-infrared peak emission frequency of a GaAs diode operating at 78 K (Dousmanis *et al.* 1964), one finds that κ is 3% for a 1.335-V bias. A detailed thermodynamic analysis of this example was conducted by Nakwaski (1982).

III. Quantitative Radiation Thermodynamics

The directional density of states (number of modes per unit volume in a frequency interval $d\nu$ and element of solid angle $d\Omega = \sin\theta d\theta d\phi$) for a beam of photons in vacuum is (Landau 1946)

$$G_{\nu, \Omega} = 2 \frac{\nu^2}{c^3} \quad (12)$$

where the factor of 2 arises from the two independent transverse polarizations of light. If the radiation propagates isotropically in all directions, then one can integrate Eq. (12) over all solid angles to obtain $G_\nu = 8\pi\nu^2 / c^3$, which is the familiar formula for the electromagnetic mode density used in the derivation of the Planck distribution (Fowles 1989) and obtained by counting the number of standing waves in a cavity. Consequently the number of modes per unit time is $cG_{\nu, \Omega} dA_\perp d\nu d\Omega$ where $dA_\perp = \cos\theta dA$ is the element of surface area dA projected into the direction of photon propagation (specified by polar and azimuthal angles θ and ϕ , respectively, in spherical coordinates) in Fig. 5. The radiation is distributed over these modes with an occupation number n (not to be confused with refractive index) that depends on ν , θ , ϕ , and the two position coordinates x and y on the surface A (which for example can be taken to span the faces of the optical cooling sample as it emits fluorescence). Multiplying the number of occupied modes per unit time by the energy $h\nu$ per photon and integrating gives the optical power,

$$\dot{E} = 2hc^{-2} \int_A \int_\Omega \int_\nu n\nu^3 d\nu \cos\theta d\Omega dA \quad (13)$$

where the overdot denotes a time derivative of the energy E carried by the beam, assumed to be unpolarized and continuous wave. The frequency and angular integrations are respectively over the spectral peaks and range of solid angles (for example, 2π in Fig. 5) relevant to the absorption or emission process of interest. A related quantity is the spectral radiance $L_\nu \equiv d\dot{E} / dA_\perp d\nu d\Omega$, sometimes called the brightness (Van Baak 1995),

$$L_\nu = \frac{2nh\nu^3}{c^2}. \quad (14)$$

The radiance is $L \equiv \int L_\nu d\nu$; in general one defines the derivative of a quantity with respect to frequency or wavelength as the corresponding ‘‘spectral’’ quantity, subscripted with ν or λ . The occupancy n determines key parameters of the radiation, including its energy and entropy fluxes

and effective temperatures. In turn, n can be obtained experimentally from Eq. (14) by measuring the spectral radiance.

The brightness temperature T_b of radiation from some source is formally defined as the temperature of a blackbody such that the spectral radiances of the Planck spectrum and of the source are equal to each other when they are averaged over some narrow range of frequencies $\delta\nu$, solid angle $\delta\Omega$, and area δA . Since blackbody photons follow the Bose-Einstein distribution (Fowles 1989), Eq. (14) therefore implies that

$$\int_{\delta A} \int_{\delta\Omega} \int_{\delta\nu} n\nu^3 d\nu \cos\theta d\Omega dA = \int_{\delta A} \int_{\delta\Omega} \int_{\delta\nu} \frac{\nu^3}{\exp(h\nu/kT_b) - 1} d\nu \cos\theta d\Omega dA. \quad (15)$$

For narrowband radiation with a central frequency $\nu_0 = c/\lambda_0$ such as might be emitted by an LED or laser whose average spectral radiance is $\bar{L}_\nu \equiv L/\Delta\nu$ where $\Delta\nu$ is the bandwidth of the radiation, Eq. (14) implies that the average photon occupation number is $\bar{n} \approx c^2 \bar{L}_\nu / 2h\nu_0^3$.

Substituting this result into Eq. (15) leads to a mean brightness temperature of

$$\bar{T}_b \approx \frac{h\nu_0}{k \ln(1 + 1/\bar{n})}, \quad (16)$$

which is therefore determined by the peak frequency and mean occupation number. For a very bright source, Eq. (16) reduces to the particularly simple form $k\bar{T}_b \approx \bar{n}h\nu_0 \approx \lambda_0^2 \bar{L}_\nu / 2$. If the radiation is emitted from an area A into a circular cone of divergence half-angle δ then the spectral radiance averaged over area, frequency, and angles is

$$\bar{L}_\nu = \frac{\dot{E}}{2\pi\delta \int_0^\delta \int_0^{2\pi} \int_0^A \int_0^{\Delta\nu} \cos\theta dA d\nu \sin\theta d\theta d\phi} = \frac{\dot{E}}{A\Delta\nu\pi\sin^2\delta}. \quad (17)$$

For example, an unpolarized 1 mW red helium-neon laser with a beam area of 1 mm², a divergence of 0.5 mrad corresponding to a solid angle of approximately $\pi\delta^2 = 0.8 \mu\text{sr}$, and a bandwidth of 1 GHz has a mean brightness temperature of 2×10^{10} K. Assuming Gaussian spectral and angular profiles with cylindrical symmetry, the detailed variation of T_b with θ and ν has been plotted in Fig. 2 of Essex *et al.* (2003). For uniform emission over a hemisphere ($\delta = \pi/2$), note that Eq. (17) becomes $\dot{E}/A\Delta\nu\pi$ and not $\dot{E}/A\Delta\nu 2\pi$ as one might have naively assumed by dividing the optical power \dot{E} by the emitting surface area A , the frequency bandwidth $\Delta\nu$, and the solid angle 2π of half of a sphere. This factor of 2 difference is a result of Lambert's cosine law (Nicodemus 1965).

Before continuing, it is appropriate to consider in more detail how to characterize a spectral quantity F_λ such as radiance or flux, illustrated in Fig. 6. The dominant wavelength λ_0 is defined to be the centroid of the spectrum,

$$\lambda_0 = \frac{\int \lambda F_\lambda d\lambda}{\int F_\lambda d\lambda}. \quad (18)$$

Noting that $F_\lambda d\lambda = F_\nu d\nu$, then in the case of the spectral energy flux density $I_{E\lambda} \equiv d\dot{E} / dA d\lambda$ (loosely called the “intensity” when a single-beam scan is recorded by a spectrometer), the mean fluorescence photon frequency is

$$\nu_F \equiv \frac{\int \nu (I_{E\nu} / h\nu) d\nu}{\int (I_{E\nu} / h\nu) d\nu} \Rightarrow \nu_F^{-1} = \frac{\int \nu^{-1} I_{E\nu} d\nu}{\int I_{E\nu} d\nu} \quad (19)$$

because $I_{E\nu} / h\nu$ is the photon spectral flux density in SI units of $\text{s}^{-1}\text{m}^{-2}\text{Hz}^{-1}$ (Mungun 2003). By inspection, the second equality is seen to agree with Eq. (18) when $F_\lambda = I_{E\lambda}$ and $\lambda_0 \equiv \lambda_F = c / \nu_F$. For a narrowband fluorescence spectrum, however, only a small error is made if one instead writes Eq. (18) with λ replaced by ν , which is equivalent to “canceling” the two factors of $h\nu$ in the first equality or the reciprocals in the second equality of Eq. (19). Next, if we define F_0 to be the maximum value of F_λ (after suitable smoothing or averaging) then $\Delta\lambda$ can be defined so that the peak–bandwidth product is

$$F_0 \Delta\lambda = \int F_\lambda d\lambda. \quad (20)$$

Let’s apply these ideas to the fluorescence emitted by an $\text{Yb}^{3+}:\text{ZBLAN}$ optical cooler pumped with $\dot{E}_p = 40 \text{ W}$ (Mungun 2005). The fluorescence power is $\dot{E}_F = (1 + \kappa)\dot{E}_p \approx \dot{E}_p$ since the coefficient of performance κ that has been experimentally observed is at most 3%. We take the cooling sample to be cylindrical with a length of 3 cm and a radius of 1.5 cm, so that its surface area is $A_{\text{sample}} = 13.5\pi \text{ cm}^2$. The fluorescence spectrum at room temperature is similar in appearance to Fig. 6(c) and is experimentally observed to have a mean wavelength of $\lambda_F = 995 \text{ nm}$ and a bandwidth of $\Delta\lambda_F = 35 \text{ nm}$ computed from Eq. (20) as the integral of the normalized spectral irradiance (also called the lineshape profile g),

$$\Delta\lambda = \int \frac{I_{E\lambda}}{I_{E0}} d\lambda \equiv \int g(\lambda) d\lambda. \quad (21)$$

Noting that frequency is related to vacuum wavelength by $\nu = c / \lambda$, it follows that $d\nu = -c d\lambda / \lambda^2$ in magnitude and hence for narrowband light that

$$\frac{\Delta\lambda}{\lambda_0} = \frac{\Delta v}{v_0} \quad (22)$$

from which one concludes that $\Delta v_F = c\Delta\lambda_F / \lambda_F^2$. Substituting this result and Eq. (17) into the average of Eq. (14) then implies that

$$\bar{n}_F = \frac{\lambda_F^5 \dot{E}_F}{2\pi hc^2 \Delta\lambda_F A_{\text{sample}}} \quad (23)$$

assuming the fluorescence is emitted homogeneously and hemispherically from the sample surface, although the detailed distribution of the light is actually nonuniform as analyzed by Chen *et al.* (2003) using ray tracing. Inserting the numbers given above, one then finds the moderately small value $\bar{n}_F = 7 \times 10^{-4}$ and when this is substituted into Eq. (16) a fluorescence brightness temperature of 2000 K is calculated. The physical significance of this result can be understood from Fig. 7 which compares the spectral radiance of a blackbody (BB),

$$L_\lambda^{\text{BB}} = \frac{2hc^2 / \lambda^5}{\exp(hc / kT_b \lambda) - 1} \quad (24)$$

at a temperature of $T_b = 2000$ K, with that of the fluorescence idealized as a single Gaussian,

$$L_\lambda = L_0 \exp\left[-\frac{1}{2}\left(\frac{\lambda - \lambda_0}{w}\right)^2\right]. \quad (25)$$

The peak value L_0 and the spectral width w corresponding to one standard deviation can be obtained by rewriting Eq. (21) in two different ways after substituting $I_{E\lambda}/I_{E0} = L_\lambda/L_0$ into it. On the one hand, we have

$$\Delta\lambda = \frac{\bar{L}_\lambda \Delta\lambda}{L_0} \Rightarrow L_0 = \frac{\dot{E}_F}{\pi \Delta\lambda_F A_{\text{sample}}} \quad (26)$$

using Eq. (17) to get the second equality. [The fact that the peak and mean values are equal is simply a consequence of the operational definition of the average of a spectral quantity given above, $\bar{L}_\lambda \equiv \int L_\lambda d\lambda / \Delta\lambda$. Theoretically it is preferable to integrate the numerator over the entire spectrum, rather than just over the bandwidth as in Ruan *et al.* (2007), because the result can then be related to the oscillator strength.] On the other hand, we can integrate Eq. (25) over all wavelengths to conclude that

$$\Delta\lambda = w\sqrt{2\pi} \approx 2w\sqrt{2\ln 2} \quad (27)$$

where the last expression defines the full-width-at-half-maximum (FWHM) of the Gaussian, in agreement with an inspection of Fig. 6(a). Therefore $w = \Delta\lambda_F / \sqrt{2\pi}$. As illustrated in Fig. 7, the

upshot is that one can find the brightness temperature of a narrowband source by plotting its spectral radiance and determining the blackbody curve that passes through its peak.

In contrast to the brightness temperature, computation of the flux temperature requires that one first calculate the rate \dot{S} at which entropy is carried by the radiation. Start by defining a (macro) state of a system of photons as consisting of N_1 photons in optical mode 1, N_2 photons in optical mode 2, and so on, not to be confused with the population densities elsewhere in this chapter. (For the moment, we are treating the modes as though they were discrete. At the end of the calculation, we will generalize the result to a continuous distribution.) Here an optical mode is defined by a particular set of values of ν , θ , ϕ , x , and y as discussed prior to Eq. (13). Now consider some ensemble of a large number M of systems (Essex *et al.* 2003). The entropy of the entire ensemble is MS . The probability that we find the system in some particular state is $P_{\text{state}} \equiv P(N_1, N_2, \dots)$. Therefore the number of systems we will find in that state is $m_{\text{state}} = MP_{\text{state}}$. If we label the states of the system by A, B, \dots then the number of ways that the systems can be arranged to form the given ensemble is

$$W = \frac{M!}{m_A!m_B!\dots} \quad (28)$$

Hence the entropy of this ensemble of systems is

$$MS = k \ln W \approx k \left[M \ln M - \sum_{\text{states}} m_{\text{state}} \ln m_{\text{state}} \right] \quad (29)$$

using Stirling's approximation in the second step. (The sum need only run over *accessible* states. Stirling's approximation for $m_{\text{state}}!$ is then always valid by choosing M large enough.)

Substituting $m_{\text{state}} = MP_{\text{state}}$ and noting that the summation of P_{state} over all possible states of the system must be unity, we conclude that

$$S = -k \sum_{\text{states}} P_{\text{state}} \ln P_{\text{state}} = -k \sum_{N_1=0}^{\infty} \sum_{N_2=0}^{\infty} \dots P(N_1, N_2, \dots) \ln P(N_1, N_2, \dots) \quad (30)$$

which is called the Shannon entropy (Carter 2001) of the system of photons. Next assume that the probability $p_i(N_i)$ of finding N_i photons in mode i is independent of the probability $p_j(N_j)$ of finding N_j photons in mode j if $i \neq j$ (Landsberg and Tonge 1980). In that case the probability of finding the system in a particular state is given by the product

$$P(N_1, N_2, \dots) = \prod_{i=1}^{\infty} p_i(N_i) \quad (31)$$

so that

$$\begin{aligned}
-S/k &= \sum_{N_1=0}^{\infty} \sum_{N_2=0}^{\infty} \sum_{N_3=0}^{\infty} \cdots (p_1 p_2 p_3 \cdots) (\ln p_1 + \ln p_2 + \ln p_3 + \cdots) \\
&= \sum p_1 \ln p_1 \sum p_2 \sum p_3 \cdots + \sum p_1 \sum p_2 \ln p_2 \sum p_3 \cdots + \sum p_1 \sum p_2 \sum p_3 \ln p_3 \cdots + \cdots.
\end{aligned} \tag{32}$$

But each summation over p_i alone is equal to unity by the normalization condition,

$$\sum_{N_i=0}^{\infty} p_i(N_i) = 1. \tag{33}$$

Therefore Eq. (32) can be tidily expressed as

$$S = \sum_{i=1}^{\infty} S_i \tag{34}$$

where the partial entropy (Ruan *et al.* 2007) of mode i is

$$S_i \equiv -k \sum_{N_i=0}^{\infty} p_i(N_i) \ln p_i(N_i). \tag{35}$$

This result states that the entropy of electromagnetic radiation is a sum of the Shannon entropy of each optical mode. To continue, let's further assume that the probability of finding one additional photon in a mode is independent of the number of photons already occupying that particular mode. This assumption implies that

$$p_i(N_i) \propto q_i^{N_i} \tag{36}$$

where q_i is the relative probability of finding one more photon in mode i . The normalization of Eq. (36) according to Eq. (33) becomes a geometric series, resulting in

$$p_i(N_i) = (1 - q_i) q_i^{N_i}. \tag{37}$$

But the (mean) occupation number of mode i is

$$n_i = \sum_{N_i=0}^{\infty} N_i p_i(N_i) = (1 - q_i) q_i \frac{d}{dq_i} \sum q_i^{N_i} = \frac{q_i}{1 - q_i}. \tag{38}$$

For example, q_i is equal to $\exp(-h\nu_i / kT)$ for radiation in thermal equilibrium at temperature T (owing to the equal spacing of the energy levels of the blackbody oscillators with which the radiation interacts), so that the (average) number of photons in mode i becomes

$$n_i = \frac{1}{\exp(h\nu_i / kT) - 1}. \tag{39}$$

Dropping the subscript i , this result is the familiar Planck occupation number (Loudon 1990) used in Eq. (15) above.

Returning to the general case of nonequilibrium radiation, Eq. (38) can be inverted to give

$$q_i = \frac{n_i}{1 + n_i}. \quad (40)$$

Substituting this result into Eq. (37) and then that into Eqs. (34)–(35), one obtains

$$\begin{aligned} S &= -k \sum_{i=1}^{\infty} \sum_{N_i=0}^{\infty} \frac{n_i^{N_i}}{(1+n_i)^{N_i+1}} \ln \frac{n_i^{N_i}}{(1+n_i)^{N_i+1}} \\ &= k \sum_{i=1}^{\infty} \sum_{N_i=0}^{\infty} \frac{(N_i+1)n_i^{N_i}}{(1+n_i)^{N_i+2}} (1+n_i) \ln(1+n_i) - k \sum_{i=1}^{\infty} \sum_{N_i=1}^{\infty} \frac{N_i n_i^{N_i-1}}{(1+n_i)^{N_i+1}} n_i \ln n_i. \end{aligned} \quad (41)$$

Let $N = N_i$ in the first summation and $N = N_i - 1$ in the second one to get

$$S = k \sum_{i=1}^{\infty} [(1+n_i) \ln(1+n_i) - n_i \ln n_i] \left\{ \frac{1}{(1+n_i)^2} \frac{d}{dq_i} \sum_{N=0}^{\infty} q_i^{N+1} \right\} \quad (42)$$

where the quantity in the curly brackets equals unity. Therefore the partial entropy for one mode of occupation number n is $k[(1+n) \ln(1+n) - n \ln n]$. Finally, as in the computation of Eq. (13), we multiply this result by $cG_{\nu, \Omega} dA_{\perp} dv d\Omega$ and integrate to find

$$\dot{S} = 2kc^{-2} \int_A \int_{\Omega} \int_{\nu} [(1+n) \ln(1+n) - n \ln n] v^2 dv \cos \theta d\Omega dA \quad (43)$$

which is called the entropy flux.

For narrowband radiation that is independent of the angular directions of propagation θ and ϕ within a circular cone of half-angle δ , then its energy flux density $I_E \equiv d\dot{E} / dA$ is

$$I_E \approx 2\pi hc^{-2} \bar{n} v_0^3 \Delta v \sin^2 \delta \quad (44)$$

from Eq. (13), while its entropy flux density $I_S \equiv d\dot{S} / dA$ using Eq. (43) is

$$I_S \approx 2\pi kc^{-2} [(1+\bar{n}) \ln(1+\bar{n}) - \bar{n} \ln \bar{n}] v_0^2 \Delta v \sin^2 \delta. \quad (45)$$

Because the thermodynamic definition of temperature is $1/T \equiv \partial S / \partial E$ at constant volume which we can take to be that of the sample considered as an “optical converter” of radiation from one form into another (Landsberg and Tonge 1980), it follows that

$$T = \frac{dI_E}{dI_S} = \frac{h\nu_0 d\bar{n}}{k \ln(1 + 1/\bar{n}) d\bar{n}} = \bar{T}_b \quad (46)$$

using Eq. (16) in the last step. Thus the brightness temperature is an absolute thermodynamic temperature even for nonequilibrium radiation.

If either the bandwidth $\Delta\nu$ or the divergence δ of the light approaches zero in a manner such that its energy flux density remains finite, then Eq. (44) requires that the mean occupation number $\bar{n} \rightarrow \infty$. In these limits, Eq. (45) becomes

$$I_S \approx \frac{k}{h\nu_0} I_E \frac{\ln \bar{n}}{\bar{n}} \rightarrow 0. \quad (47)$$

That is, if the radiation crossing a differential area dA is either monochromatic or unidirectional as illustrated in Fig. 8, then the beam carries zero entropy. In this sense, one can characterize an ideal laser beam as purely doing work to drive an optical cooler, in striking contrast to blackbody radiation which only delivers heat (Mungan 2005). Note however from Eq. (46) that $\int T dI_S$ is always equal to the irradiance and does *not* define a heat flux density for nonequilibrium radiation.

The flux temperature of radiation is now defined as

$$T_f \equiv \frac{I_E}{I_S} \quad (48)$$

which should be carefully contrasted with Eq. (46). For narrowband light this definition becomes

$$T_f \approx \frac{h\nu_0 \bar{n}}{k[(1 + \bar{n})\ln(1 + \bar{n}) - \bar{n} \ln \bar{n}]} \quad (49)$$

using Eqs. (44) and (45). In accord with the discussion of Eq. (47) this flux temperature becomes infinite as $\bar{n} \rightarrow \infty$, consistent with the fact that an ideal laser beam carries zero entropy at a finite irradiance. Equations (49) and (16) are plotted in Fig. 9 for 1- μm radiation, using Eq. (14) to relate the mean photon occupation number and spectral radiance. When $\bar{n} \ll 1$ these two temperatures become

$$\bar{T}_b \approx \frac{h\nu_0 / k}{\ln(1 / \bar{n})} \quad \text{and} \quad T_f \approx \frac{h\nu_0 / k}{1 + \ln(1 / \bar{n})} \quad (50)$$

which leads to the simple formula

$$(kT_f)^{-1} \approx (k\bar{T}_b)^{-1} + (h\nu_0)^{-1}. \quad (51)$$

Using the values $\lambda_F = 995 \text{ nm}$ and $\bar{T}_b = 2000 \text{ K}$ for $\text{Yb}^{3+}:\text{ZBLAN}$ given in connection with Eq. (23), this formula results in a fluorescence flux temperature of $T_f = 1750 \text{ K}$. Note that Eq. (50) implies that $T_f \rightarrow \bar{T}_b$ as $\bar{n} \rightarrow 0$, i.e., the flux and brightness temperatures become equal for sufficiently dim, narrowband radiation as one can see in Fig. 9. In contrast $I_E^{\text{BB}} = \sigma T_b^4$ and

$I_S^{\text{BB}} = \frac{4}{3}\sigma T_b^3$ for blackbody radiation (where $\sigma = 2\pi^5 k^4 / 15c^2 h^3$ is the Stefan-Boltzmann constant), so that $T_f = 0.75T_b$ according to Eq. (48). This result states that if an isothermal body of unit emissivity radiates away heat Q into free space, then while the object loses entropy Q/T , the thermal radiation carries away entropy $4Q/3T$. The net entropy change for this irreversible emission process in a zero-kelvin environment is positive; entropy is only conserved if the surroundings are instead infinitesimally smaller in temperature than the body (Mungan 2005).

IV. Ideal and Actual Performance of Optical Refrigerators

Consider the fluxes of energy and entropy into and out of the cooler sketched in Fig. 10 operating at steady state. The first law of thermodynamics for this system becomes

$$\dot{E}_F = \dot{E}_P + \dot{Q}, \quad (52)$$

where \dot{E}_P is here taken to be the absorbed pump power, after correcting for reflection, scattering, and transmission losses of the incident beam. Meanwhile the second law states that

$$\dot{S}_F = \dot{S}_P + \frac{\dot{Q}}{T} + \dot{S}_G \quad (53)$$

where \dot{S}_G is the rate at which entropy is internally generated during a cooling cycle due to irreversible processes such as nonradiative relaxation, phonon equilibration, and spontaneous emission (Mungan and Gosnell 1999). Substituting Eq. (48) into (53) leads to

$$\frac{\dot{E}_F}{T_F} = \frac{\dot{E}_P}{T_P} + \frac{\dot{Q}}{T} + \dot{S}_G = \frac{\dot{E}_P + \dot{Q}}{T_F} \quad (54)$$

using Eq. (52) to get the second equality, where T_F and T_P are the flux temperatures of the fluorescence and pump radiation, respectively. This result can be rearranged to compute the coefficient of performance (COP) $\kappa \equiv \dot{Q} / \dot{E}_P$, sometimes called the cooling efficiency relative to the absorbed pump power,

$$\kappa = \frac{T - \Delta\tilde{T}}{T_F - T} \quad \text{where} \quad \Delta\tilde{T} \equiv \frac{TT_F}{T_P} \left(1 + \frac{\dot{S}_G}{\dot{S}_P} \right) = \Delta T + T \frac{T_F \dot{S}_G}{\dot{E}_P}. \quad (55)$$

Notice that the maximum value for the COP is achieved for reversible operation of the cooler when $\dot{S}_G = 0$ so that $\Delta\tilde{T} = \Delta T$, thereby reproducing the Carnot value κ_C of Eq. (4).

At the next level of approximation, assume that entropy is generated solely by nonradiative processes, such as direct multiphonon de-excitation of the active ions or energy transfer to nonfluorescent impurities. Define energy E_F to be the fluorescent photon energy $h\nu_F$ multiplied by the number of excited ions in the sample $\mathcal{N}_2 = \int N_2 dV$, where N_2 is the population density of the upper manifold, as in Eq. (67) below. The radiative and nonradiative lifetimes of the excited

state are τ_R and τ_{NR} , respectively. Then the average fluorescent power is $\dot{E}_F = E_F / \tau_R$ which escapes from the sample resulting in cooling. If that same amount of energy were to decay nonradiatively, then it would on average generate heating of $\dot{E}_H = E_F / \tau_{NR}$ which is deposited in the sample as thermal energy. (This is almost but not exactly equal to the actual nonradiative power which is $\dot{E}_{NR} = \mathcal{N}_2 h\nu_P / \tau_{NR}$. By energy conservation, each nonradiative relaxation must on average distribute a pump photon energy among the internal phonon modes and thus the nonradiative energy per decay is $h\nu_P$, which only equals $h\nu_F$ if one pumps at the mean fluorescence wavelength.) The fluorescence quantum efficiency (QE) can now be written as

$$\eta \equiv \frac{1/\tau_R}{1/\tau_R + 1/\tau_{NR}} = \frac{\dot{E}_F}{\dot{E}_F + \dot{E}_H} \Rightarrow \dot{E}_H = \frac{1-\eta}{\eta} \dot{E}_F. \quad (56)$$

(Technically the first equality defines the *internal* QE $\eta_{\text{int}} = \tau / \tau_R$ where τ is the overall lifetime; η_{int} is only equal to the *external* QE η_{ext} if the escape probability f_{esc} is 100%. The correction for non-unit escape probability is discussed later.) Excess entropy results from the difference between dumping this thermal energy into the sample at temperature T compared to carrying that energy away on the fluorescence beam at temperature T_F (Ruan *et al.* 2007),

$$\dot{S}_G = \frac{\dot{E}_H}{T} - \frac{\dot{E}_H}{T_F} = (\dot{E}_P + \dot{Q}) \left(\frac{1-\eta}{\eta} \right) \left(\frac{1}{T} - \frac{1}{T_F} \right) \quad (57)$$

using Eqs. (52) and (56) in the second step. Substituting this result into Eq. (55) now gives

$$\kappa = (T_F - T)^{-1} \left[T - \Delta T - TT_F (1 + \kappa) \left(\frac{1-\eta}{\eta} \right) \left(\frac{1}{T} - \frac{1}{T_F} \right) \right]. \quad (58)$$

Equation (58) neatly simplifies to

$$\kappa = \eta \frac{T - \Delta T}{T_F - T} - 1 + \eta. \quad (59)$$

As a check, note that κ reduces to κ_C given by Eq. (4) when $\eta = 1$ because in this limit there is no nonradiative relaxation and hence no excess entropy generation. That Carnot expression for the COP can be used to rewrite Eq. (59) more compactly as

$$\kappa = \eta (1 + \kappa_C) - 1, \quad (60)$$

which is zero when $\eta \approx 1 - T/T_F = 83\%$ if $T = 300$ K and $T_F = 1750$ K $\gg \Delta T$ (as for Yb³⁺:ZBLAN). Letting the fluorescence QE η approach zero causes $\kappa = -1$ because 100% of the pump energy would then be converted into heat. More generally, solving Eq. (60) for κ_C and substituting into it $\kappa = \dot{Q} / \dot{E}_P$ and $\eta = (\dot{E}_P + \dot{Q}) / (\dot{E}_P + \dot{Q} + \dot{E}_H)$ from Eq. (56) using (52), one finds $\kappa_C = (\dot{Q} + \dot{E}_H) / \dot{E}_P$. This result makes sense because the numerator is the cooling power

one would obtain if the nonradiative decays were radiative instead. Alternatively, one could start from this result and work backward to obtain Eq. (57), thereby proving that nonradiative relaxation is an irreversible source of entropy.

Another interpretation of Eq. (60) comes from substituting Eq. (9) into it in the form $1 + \kappa_C = \lambda_P / \lambda_F$. One then finds

$$\kappa = \frac{\lambda_P - \lambda_F^*}{\lambda_F^*} \quad (61)$$

where $\lambda_F^* \equiv \lambda_F / \eta$ is the zero-heating wavelength corrected for nonradiative de-excitations. As expected intuitively, the effect of a non-unit fluorescence QE is to redshift further into the tail of the absorption band the minimum pump wavelength at which net cooling occurs.

Returning to the experimental cooling results for $\text{Yb}^{3+}:\text{ZBLAN}$, a titanium-sapphire pump laser is often used, which is continuous wave, narrowband, and bright so that $\bar{n} \gg 1$ in Eq. (49) and hence the pump flux temperature can be approximated as

$$T_P \approx \frac{hc\bar{n}_P}{k\lambda_P(1 + \ln\bar{n}_P)} \quad \text{with} \quad \bar{n}_P \approx \frac{\lambda_P^3 \dot{E}_P}{2hc\pi R_P^2 \Delta\nu_P \pi \delta_P^2} \quad (62)$$

where the second equality comes from Eqs. (14) and (17). Supposing the source has a power of $\dot{E}_P = 40 \text{ W}$, a beam radius of $R_P = 0.5 \text{ mm}$, a bandwidth of $\Delta\nu_P = 40 \text{ GHz}$, a divergence of $\delta_P = 1 \text{ mrad}$, and a wavelength of $\lambda_P = 1030 \text{ nm}$ (Mungan 2005) then $\bar{n}_P \approx 10^9$ so that $T_P \approx 7 \times 10^{11} \text{ K}$. In comparison, the fluorescence flux temperature T_F was computed above to be 1750 K using Eq. (51). Consequently $\Delta T / T \equiv T_F / T_P \ll 1$ and Eq. (5) becomes an excellent estimate for the Carnot COP of a laser-driven optical cooler. Then $\kappa_C = (T_F / T - 1)^{-1}$ only depends on the ratio of the fluorescence flux and refrigerating sample temperatures. This result would also hold for an electroluminescent cooler, since an electric current delivers energy E_P at near zero entropy S_P (ignoring inefficiencies such as Joule heating, Auger processes, and surface recombination) so that $T_P = E_P / S_P$ is again much larger than T_F .

So far we have only considered the interactions between the sample, pump, and fluorescence. However the surroundings at ambient temperature T_A (say the inner walls of the cryostat in which the sample is suspended by low-thermal-conductivity mounts) also couple radiatively to the refrigerator (Weinstein 1960). This coupling can be reduced for a practical cryocooler by inserting a set of heat shields between the sample and the walls, as in Fig. 11. For example, for an ytterbium-based cooler mounted in a room-temperature vacuum chamber, the heat shield would be designed to transmit the $1\text{-}\mu\text{m}$ fluorescence out to the heat-sunk walls while reflecting their $10\text{-}\mu\text{m}$ thermal radiation (with corresponding blackbody photon occupation number n_A) back away from the sample. The heat shield is thus a short-wavelength-pass filter (sometimes

called a “hot mirror”). Since the cooler is presumably operating at a temperature T less than T_A , thermal radiation from the sample (with occupation number n_T) will peak at wavelengths even longer than $10 \mu\text{m}$ and will consequently be reflected back to the sample. Ignoring the pump, it therefore follows that the light incident on the cooling sample will have occupation number n_T while that leaving it will have occupation $n_F + n_T$. The net energy and entropy fluxes from the sample result from the difference between the outgoing and incoming radiation,

$$\dot{E}_{\text{net}} = 2hc^{-2} \int_A \int_{\Omega} \int_V (n_F + n_T) v^3 dv \cos \theta d\Omega dA - 2hc^{-2} \int_A \int_{\Omega} \int_V n_T v^3 dv \cos \theta d\Omega dA \quad (63)$$

which simplifies back to Eq. (13) with n identified as n_F , while

$$\begin{aligned} \dot{S}_{\text{net}} = & 2kc^{-2} \int_A \int_{\Omega} \int_V [(1 + n_F + n_T) \ln(1 + n_F + n_T) - (n_F + n_T) \ln(n_F + n_T)] v^2 dv \cos \theta d\Omega dA \\ & - 2kc^{-2} \int_A \int_{\Omega} \int_V [(1 + n_T) \ln(1 + n_T) - n_T \ln n_T] v^2 dv \cos \theta d\Omega dA \end{aligned} \quad (64)$$

does *not* reduce to Eq. (43) when n is similarly identified. Unlike energy, the entropy of a beam of light is not additive over photons that share the same mode (in particular, the same frequency). This fact means that the entropy of the sample’s emission depends on the temperature of the thermal surroundings. In particular, in the limit of very weak fluorescence $n_F \ll n_T$, we can neglect n_F in the arguments of the first two logarithms in Eq. (64) to get

$$\dot{S}_{\text{net}} \approx 2kc^{-2} \int_A \int_{\Omega} \int_V n_F \ln(1 + 1/n_T) v^2 dv \cos \theta d\Omega dA. \quad (65)$$

But $\ln(1 + 1/n_T) = hv/kT$ from Eq. (39) and thus $\dot{S}_{\text{net}} = \dot{E}_{\text{net}}/T \Rightarrow T_F \rightarrow T$. This result keeps the Carnot coefficient of performance in Eq. (5) positive regardless of how weak the fluorescence gets. In fact, as the pump power (and hence the resulting fluorescence) is reduced, κ_C increases as graphed by the left-hand curve in Fig. 12, diverging as $\dot{E}_p \rightarrow 0$. The reason the COP becomes infinite in this limit is that the sample will still cool back to the ambient temperature if it is impulsively heated, so that there is a nonzero cooling power even though the pump power is zero, owing to the sample’s radiative coupling to the surroundings (arising from a small leakage of thermal radiation through the heat shield in Fig. 11 at short wavelengths). One can equivalently think of this as thermally stimulated fluorescence. Needless to say, the fact that κ_C increases with decreasing \dot{E}_p does not imply that there is some maximum in the cooling power of an ideal optical refrigerator at low or intermediate pump powers. On the contrary, for a cooler operating at the Carnot limit, Eq. (53) implies that $\dot{Q}/T = \dot{S}_F$ (assuming the entropy of the pump is negligible), which is plotted as the right-hand curve in Fig. 12 for narrowband ytterbium fluorescence and rises monotonically with pump power.

Equation (65) is only valid if the fluorescence is extremely weak. Specifically, when $T = 300 \text{ K}$ and $c/\nu = 995 \text{ nm}$, Eq. (39) gives $n_T = 10^{-21}$. Using the previous values of the

material constants, Eq. (23) implies that $\bar{n}_F = n_T$ only when the fluorescence power has the tiny value $\dot{E}_F = 10^{-16}$ W. Clearly we can assume that $n_F \gg n_T$ within the ytterbium spectral range whenever the optical fridge is operating. In this limit of small n_T , the quantity in square brackets in the second integral of Eq. (64) becomes approximately $(-\ln n_T)/(1/n_T) \approx 0$ using l'Hôpital's rule. Therefore Eq. (64) now *does* simplify to Eq. (43) with n identified as n_F .

With that conclusion in mind, the graphs in Fig. 12 were computed as follows. A value of the fluorescence occupation number \bar{n}_F was picked and \dot{E}_F was computed from it using Eq. (23). Similarly the fluorescence entropy flux was calculated as

$$\dot{S}_F = 2\pi k c A_{\text{sample}} \left[(1 + \bar{n}_F) \ln(1 + \bar{n}_F) - \bar{n}_F \ln \bar{n}_F \right] \lambda_F^{-4} \Delta \lambda_F \quad (66)$$

from Eq. (45). Then the fluorescence flux temperature was found from their ratio, $T_F \equiv \dot{E}_F / \dot{S}_F$, and it was substituted into Eq. (5) to determine κ_C . Finally the pump power could be determined as $\dot{E}_P = \dot{E}_F / (1 + \kappa_C)$ using Eq. (52), so that κ_C and \dot{S}_F could be plotted one point at a time against \dot{E}_P . Unlike κ_C whose value depends critically on the sample temperature T , assumed to be room temperature in Fig. 12, \dot{Q}/T as given by Eq. (66) only depends weakly on T , via the temperature dependences of λ_F and $\Delta \lambda_F$ measured by Lei *et al.* (1998), noting from the two graphs in Fig. 12 that $\dot{E}_P \approx \dot{E}_F$ when the pump is strong enough to give significant cooling. Also note that the right-hand plot of \dot{Q}/T versus $\log \dot{E}_P$ becomes linear at high powers because then $\dot{S}_F \propto \ln \bar{n}_F$ from Eq. (66) while $\dot{E}_P \approx \dot{E}_F \propto \bar{n}_F$.

The current lowest temperature experimentally attained by optical cooling is $T = 208$ K for a 2 wt% Yb³⁺:ZBLAN cylindrical sample starting from room temperature (Thiede *et al.* 2005). The mean fluorescence wavelength at this temperature is $\lambda_F = 999$ nm and the bandwidth is approximately the same as its room temperature value of $\Delta \lambda_F = 35$ nm. Since the end faces of the sample were coated with high reflectors that substantially reduce fluorescence escape from them, it is reasonable to estimate the sample area only by that of the curved surface, specifically of the outer cladding (since $\delta = \pi/2$ for it) so that $A_{\text{sample}} = 88\pi \text{ mm}^2$. The sample was pumped using an Yb³⁺:YAG laser with an absorbed power of $\dot{E}_P = 5.9$ W $\approx \dot{E}_F$ (assuming 61% absorptance) at a wavelength of $\lambda_P = 1026$ nm for 3 hours (to reach steady state). Consequently Eq. (23) implies that the mean fluorescence occupation number is $\bar{n}_F = 1.6 \times 10^{-3}$, corresponding to a flux temperature of $T_F = 1900$ K from Eq. (50). The sample and flux temperatures then lead to a Carnot COP of $\kappa_C = 12\%$ according to Eq. (5). For comparison, the coefficient of performance predicted spectroscopically is $\kappa_C = 2.7\%$ from Eq. (9). However the heat load at the minimum temperature was found to be $\dot{Q} = 29$ mW and thus the actual COP is just $\kappa = \dot{Q} / \dot{E}_P = 0.5\%$.

Another sample for which more than 10°C of cooling has been observed is Tm³⁺:ZBLAN (Hoyt *et al.* 2003a–b). A Brewster-cut 1 wt% sample was cooled by 24 K below room

temperature (i.e., to about $T = 275$ K) by exciting it at $\lambda_p = 1.9$ μm for half an hour with an average absorbed power of $\dot{E}_p = 2.2$ W $\approx \dot{E}_F$ using an optical parametric oscillator pumped by a 25-W mode-locked Nd³⁺:YAG laser. The surface area of the sample was about $A_{\text{sample}} = 150$ mm². The fluorescence spectrum consists of a single symmetric peak centered at $\lambda_F = 1.803$ μm with a FWHM of $\Delta\lambda_F = 0.22$ μm . Using these values, one finds that $\bar{n}_F = 3.4 \times 10^{-3}$ from Eq. (23), so that $T_F = 1200$ K according to Eq. (50). Therefore Eq. (5) gives rise to $\kappa_C = 30\%$, whereas the ideal spectroscopic prediction is $\kappa_C = 5.4\%$ according to Eq. (9). Note that the latter value is double that calculated for Yb³⁺:ZBLAN above because, as discussed following Eq. (9), κ_C is approximately proportional to λ_p and for thulium we double this wavelength from about 1 to 2 μm . With an estimated cooling power of $\dot{Q} = 73$ mW, the actual COP may be as high as $\kappa = \dot{Q} / \dot{E}_p = 3.3\%$, which is promising for practical refrigeration.

To explain the differences between the thermodynamic, spectroscopic, and actual cooling coefficients of performance, we need to consider various sources of inefficiencies. Equation (61) for example indicates that κ strongly depends on the internal fluorescence quantum efficiency η_{int} . In addition, the COP is expected to depend on the probability f_{esc} that the spontaneously emitted photons escape from the sample, the background absorption coefficient α_{back} of the pump light by nonfluorescent impurities or sample surface coatings, and the saturation intensity (irradiance) I_{sat} when one pumps near an absorption peak. The following model, which extends that of Hoyt *et al.* (2003a), incorporates all four of these effects (η_{int} , f_{esc} , α_{back} , and I_{sat}).

Consider a small volume element of the sample dV at spatial position \mathbf{r} that is being optically pumped with incident intensity $I(\mathbf{r})$ in W/cm² at wavelength $\lambda_p = c / \nu_p$. The population densities (ions/cm³) in the ground and excited manifolds are N_1 and N_2 , respectively, where $N = N_1 + N_2$ is the concentration of active ions doped into the host crystal or glass and is assumed to be spatially uniform. Denote the effective absorption and emission cross sections (in cm²) at the pump wavelength as σ_{AP} and σ_{EP} , respectively, and define (Bowman and Mungan 2000) the dimensionless ratio $\beta \equiv \sigma_{\text{AP}} / (\sigma_{\text{AP}} + \sigma_{\text{EP}})$. (Note that $\beta = 0.5$ for a true two-level system.) The radiative and nonradiative rates are the inverses of the lifetimes, $W_R = 1 / \tau_R$ and $W_{\text{NR}} = 1 / \tau_{\text{NR}}$, respectively.

In steady state, a rate-equation approach leads to two key relations. First, the time dependence of the excited-state population is described by

$$\frac{dN_2}{dt} = 0 = \frac{I}{h\nu_p} (N_1\sigma_{\text{AP}} - N_2\sigma_{\text{EP}}) - f_{\text{esc}}N_2W_R - N_2W_{\text{NR}}, \quad (67)$$

assuming the pump bandwidth $\Delta\lambda_p$ is narrow enough that the wavelength dependence of the cross sections can be ignored; otherwise one needs to replace each product $I\sigma$ by $I_\lambda\sigma(\lambda)$ and integrate Eqs. (67) and (71) over wavelength. The first expression on the right-hand side of

Eq. (67) is the difference between absorption and stimulated emission, the second term describes spontaneous emission, and the last one accounts for nonradiative decay (including both direct multiphonon de-excitation and energy transfer from the excited ions to nonfluorescent impurities). The spontaneous radiation term includes the fractional probability f_{esc} that the fluorescence photons ultimately escape from the sample. Photons which do not escape are assumed to get reabsorbed by active ions (i.e., perfect photon recycling), resulting in no net change in the excited-state population; Wang *et al.* (2006) have considered the case of nonideal recycling and its effect is to further reduce the external quantum efficiency. For simplicity f_{esc} is here taken to be an average value over the entire sample; in actuality it depends on \mathbf{r} both because of the proximity of the pumped volume element to the sample surfaces and because the photons emitted in one volume element are in general absorbed in a different volume element (Heeg *et al.* 2005). In contrast, the stimulated emission photons are assumed to be added to the pump beam and so no escape fraction is needed inside the first term. Define the external fluorescence quantum efficiency (QE) as

$$\eta_{\text{ext}} \equiv \frac{f_{\text{esc}} W_{\text{R}}}{f_{\text{esc}} W_{\text{R}} + W_{\text{NR}}}, \quad (68)$$

which can be related to the internal QE η_{int} defined by the first equality in Eq. (56),

$$\eta_{\text{ext}}^{-1} - 1 = \frac{\eta_{\text{int}}^{-1} - 1}{f_{\text{esc}}}. \quad (69)$$

This expression can be used to directly compute the external QE in terms of the internal value (or vice versa) if the escape probability is known. (Note that if $f_{\text{esc}} \neq 1$, the internal and external efficiencies are only equal to each other in the limits that η approaches zero or unity.) Using Eq. (68) to eliminate W_{NR} in Eq. (67), one obtains

$$\frac{N_2}{N} = \frac{\beta}{1 + I_{\text{sat}} / I} \quad (70)$$

where the pump saturation intensity is $I_{\text{sat}} \equiv h\nu_{\text{P}} f_{\text{esc}} W_{\text{R}} / \eta_{\text{ext}} (\sigma_{\text{AP}} + \sigma_{\text{EP}})$.

The second key relation is the rate of thermal energy accumulation in the volume element,

$$\dot{u} = (N_1 \sigma_{\text{AP}} - N_2 \sigma_{\text{EP}}) I + \alpha_{\text{back}} I - f_{\text{esc}} N_2 h\nu_{\text{F}} W_{\text{R}} \quad (71)$$

in W/cm^3 , where α_{back} is an average background nonsaturable absorption coefficient (in cm^{-1}) which is assumed to be approximately wavelength independent due to nonfluorescent impurities and surface coatings, and $\nu_{\text{F}} = c / \lambda_{\text{F}}$ is the mean fluorescence frequency including the redshifting due to reabsorption. The redshift can be calculated from the overlap between the absorption and emission spectra; for example, Lamouche *et al.* (1998) estimate a +9 nm shift for

a 2% Yb³⁺:ZBLAN sample measuring 3 cm on a side. Noting that the resonant absorption coefficient by the active ions is $\alpha_{\text{res}} = N\sigma_{\text{AP}}$ and defining the total absorption coefficient as $\alpha_{\text{tot}} = \alpha_{\text{res}} + \alpha_{\text{back}}$, we can use Eq. (70) to rewrite Eq. (71) in dimensionless form as

$$\frac{\dot{u}}{\alpha_{\text{tot}} I} = 1 - \frac{\eta_{\text{ext}} \lambda_{\text{P}} / \lambda_{\text{F}} + I / I_{\text{sat}}}{1 + I / I_{\text{sat}}} \frac{\alpha_{\text{res}}}{\alpha_{\text{tot}}}. \quad (72)$$

The numerator of the left-hand side is the net heating power density while the denominator is the total absorbed power density. Therefore the negative of this expression defines the cooling COP which can be rewritten in the form

$$\kappa = \frac{\lambda_{\text{P}} - \lambda_{\text{F}}^*}{\lambda_{\text{F}}^{**}}. \quad (73)$$

Here the zero-heating wavelengths are

$$\lambda_{\text{F}}^* = \frac{\lambda_{\text{F}}}{\eta_{\text{ext}}} \left(\frac{\alpha_{\text{tot}} + \alpha_{\text{back}} I / I_{\text{sat}}}{\alpha_{\text{res}}} \right) \quad (74)$$

while the slope of a graph of κ versus λ_{P} (as in Fig. 14 introduced below) is normalized by

$$\lambda_{\text{F}}^{**} = \frac{\lambda_{\text{F}}}{\eta_{\text{ext}}} \left(1 + \frac{I}{I_{\text{sat}}} \right) \frac{\alpha_{\text{tot}}}{\alpha_{\text{res}}}. \quad (75)$$

As a check, Eq. (73) reduces to Eq. (61) when $f_{\text{esc}} = 1$ (so that the internal and external quantum efficiencies are equal), $\alpha_{\text{back}} = 0$ (so that the pump light is only absorbed by the active ions), and $I_{\text{sat}} \rightarrow \infty$ (so that the absorption by the active ions cannot be saturated). More realistically $I_{\text{sat}} = 15 \text{ kW/cm}^2$ if Yb³⁺:ZBLAN is pumped at $\lambda_{\text{P}} = 1 \mu\text{m}$ so that $\sigma_{\text{AP}} + \sigma_{\text{EP}} \approx 5 \times 10^{-21} \text{ cm}^2$ at room temperature, assuming values of $f_{\text{esc}} = 75\%$, $\tau_{\text{R}} = 2 \text{ ms}$, and $\eta_{\text{ext}} = 99\%$. This irradiance would be attained by a 1-W pump beam having a diameter of about 0.1 mm, and therefore it is not surprising that one sees saturation effects when performing focused photothermal deflection spectroscopic measurements or when the cooling sample is a piece of an optical fiber (Mungan and Gosnell 1999). In either case, the result is to reduce the amount of laser heating or cooling observed, since both λ_{F}^* and λ_{F}^{**} increase with increasing pump intensity I in Eqs. (74) and (75). As an example, the ratio of the COP to its unsaturated value has been plotted in Fig. 13 as a function of the pump intensity for the case of $\alpha_{\text{back}} = 0$.

Owing to such saturation effects, the right-hand curve of the cooling power in Fig. 12 must roll over at high pump powers, rather than continuing to increase without limit, although a “top hat” spatial profile of the laser beam can help delay that onset. In any event, the cooling rate is ultimately limited to $1 / \tau_{\text{R}} = 500 \text{ Hz}$ per ytterbium ion.

On the other hand, in the limit of weak pumping ($I \ll I_{\text{sat}}$) which will always occur at sufficiently long wavelengths, Eqs. (74) and (75) become $\lambda_{\text{F}}^* = \lambda_{\text{F}}^{**} = \lambda_{\text{F}} / (\gamma \eta_{\text{ext}})$ where the absorption efficiency (Sheik-Bahae and Epstein 2007) is $\gamma \equiv \alpha_{\text{res}} / \alpha_{\text{tot}}$. The resulting expression for κ from Eq. (73) has been plotted in Fig. 14 using values of the numerical constants representative of purified $\text{Yb}^{3+}:\text{ZBLAN}$ material, assuming a sample geometry such that fluorescence reabsorption is negligible and estimating the ytterbium absorption coefficient as

$$\alpha_{\text{res}}(\lambda_{\text{p}}) = (0.36 \text{ cm}^{-1}) \exp \left[- \left(\frac{\lambda_{\text{p}} - 975 \text{ nm}}{33 \text{ nm}} \right)^2 \right] \quad (76)$$

which was fit to the 300 K reciprocity-derived spectrum of a 1% doped sample over the range 990–1060 nm (Lei *et al.* 1998). We see from this graph that the cooling range is bracketed by two zero-heating wavelengths. At short pump wavelengths, α_{back} is negligible compared to α_{res} and Eq. (73) becomes

$$\kappa = \frac{\lambda_{\text{p}} - \lambda_{\text{F}} / \eta_{\text{ext}}}{\lambda_{\text{F}} / \eta_{\text{ext}}} = \frac{\dot{E}_{\text{F}}}{\dot{E}_{\text{F}} \lambda_{\text{F}} / \lambda_{\text{p}} + \dot{E}_{\text{NR}}} - 1. \quad (77)$$

The first equality is identical to Eq. (61) with the internal fluorescence QE replaced by the external QE, and thus κ rises linearly with λ_{p} and crosses zero near $\lambda_{\text{F}} / \eta_{\text{ext}} = 1005 \text{ nm}$. The second equality follows by substituting Eq. (68) and defining the external fluorescence power by $\dot{E}_{\text{F}} = f_{\text{esc}} \mathcal{N}_2 h \nu_{\text{F}} / \tau_{\text{R}}$ and the nonradiative heating by $\dot{E}_{\text{NR}} = \mathcal{N}_2 h \nu_{\text{P}} / \tau_{\text{NR}}$ as discussed before Eq. (56). Some quick checks on any purported expression for the cooling coefficient κ (of which there have been many in the literature) are that $\kappa = -1$ if $\tau_{\text{R}} \rightarrow \infty$ or if $f_{\text{esc}} = 0$ (in which case the best you can do is locally cool one region of the sample and distribute the heat elsewhere, assuming the material's thermal conductivity is low enough to support such a gradient), and that $\kappa = \kappa_{\text{C}}$ from Eq. (9) in the absence of saturation and all nonradiative heating (such as from background or excited-state absorption, multiphonon relaxation, and energy transfer). Equation (77) satisfies these checks when one sets \dot{E}_{F} or \dot{E}_{NR} to zero, respectively. Note that the denominator of the second equality can be written as

$f_{\text{esc}} \mathcal{N}_2 h \nu_{\text{P}} / \tau_{\text{R}} + \mathcal{N}_2 h \nu_{\text{P}} / \tau_{\text{NR}} = \mathcal{N}_2 h \nu_{\text{P}} / \tau_{\text{ext}}$, where τ_{ext} is the external lifetime of the active ions, which is longer than the the internal value owing to radiative trapping of the fluorescence. But $\mathcal{N}_2 h \nu_{\text{P}} / \tau_{\text{ext}}$ equals the absorbed pump power \dot{E}_{P} in steady state. Equation (77) can then be immediately recognized as the expected ratio of the cooling to the absorbed power.

On the other hand as one tunes to long wavelengths, $\alpha_{\text{res}}(\lambda_{\text{p}})$ declines in value while α_{back} is assumed constant, so that the cooling COP does not continue to increase but instead bends over, returning to zero when $\alpha_{\text{res}}(\lambda_{\text{p}}) = \alpha_{\text{back}} / (\eta_{\text{ext}} \lambda_{\text{p}} / \lambda_{\text{F}} - 1)$. Substituting Eq. (76), this second

zero-heating pump wavelength is found at 1049 nm. The peak cooling in Fig. 14 occurs near $\lambda_p = 1036$ nm, in reasonable agreement with experimental results (Edwards *et al.* 1999).

V. Closing Remarks

This chapter has focused on calculating the coefficient of performance (COP) κ . Many workers in the field of optical cooling prefer to report quantities other than the COP, which are related to it. The cooling power P_{cool} equals the product of κ and the absorbed pump power $P_{\text{abs}} = \dot{E}_p$. In the unsaturated limit, the absorbed power in turn is the product of the incident power P_{inc} and the absorptance $1 - \exp(-\alpha_{\text{res}}L)$ where L is the sample length (multiplied by the number of passes if it is in a cavity). For a short sample in single-pass pumping, one can therefore approximate $P_{\text{abs}} \approx \alpha_{\text{res}}LP_{\text{inc}}$. Once the steady-state refrigeration temperature T has been attained, the cooling power is equal to the heat load, $P_{\text{cool}} = \dot{Q}$. If the load is thermal radiation from a surrounding chamber (possibly coated with a heat-shielding material) of internal surface area A_c at temperature T_c with an emissivity of ϵ_c then (Clark *et al.* 1998)

$$\dot{Q} = \frac{\sigma(T_c^4 - T^4)}{(A\epsilon)^{-1} + (1 - \epsilon_c)(A_c\epsilon_c)^{-1}} \quad (78)$$

where the cooling sample has surface area A and emissivity ϵ . An upper limit on the heat load is obtained by putting $\epsilon_c = 1 = \epsilon$. If furthermore the cooler is operating at a temperature $T = T_c - \delta T$ where δT is small, then $\dot{Q} \approx 4A\sigma T_c^3 \delta T$. Suppose the sample is in the form of an optical fiber of small diameter D , so that $A \approx \pi DL$. Then the COP becomes

$$\kappa \equiv \frac{\dot{Q}}{P_{\text{abs}}} \approx \frac{4\pi\sigma DT_c^3 \delta T}{\alpha_{\text{res}}P_{\text{inc}}} \quad (79)$$

so that, ideally using Eq. (9), the temperature drop normalized to the incident laser power is

$$\frac{\delta T}{P_{\text{inc}}} = \frac{N}{4\pi\sigma DT_c^3} F_{\text{cool}} \quad (80)$$

where N is the concentration of active ions and the cooling figure of merit (Bowman and Mungan 2000) is $F_{\text{cool}} \equiv \sigma_{\text{AP}}(\lambda_p - \lambda_F) / \lambda_F$ at the optimal pump wavelength λ_p , which is useful for comparing the cooling potential of different materials. Equation (80) suggests possible strategies for maximizing the temperature drop, such as increasing the Yb^{3+} doping (until energy transfer becomes limiting) and decreasing the sample diameter (so that its entire cross section is pumped).

From a spectroscopic point of view, the ratio of the external radiative relaxation rate to the total decay rate of the upper state defines the fluorescence quantum efficiency (QE),

$$\eta_{\text{ext}} \equiv \frac{f_{\text{esc}} / \tau_{\text{R}}}{1 / \tau_{\text{ext}}} \quad (81)$$

where $1 / \tau_{\text{ext}} \equiv f_{\text{esc}} / \tau_{\text{R}} + 1 / \tau_{\text{NR}}$. But the ratio of the external fluorescent power \dot{E}_{F} to the absorbed pump power defines the cooling coefficient of performance (COP) plus unity,

$$\kappa + 1 \equiv \frac{f_{\text{esc}} \mathcal{N}_2 h \nu_{\text{F}} / \tau_{\text{R}}}{\mathcal{N}_2 h \nu_{\text{P}} / \tau_{\text{ext}}} \quad (82)$$

in the absence of both saturation and background absorption. (Note that photon recycling will be perfect in this case because nothing other than active ions can reabsorb the fluorescent light.)

Thus $\kappa + 1 = \eta_{\text{ext}} \nu_{\text{F}} / \nu_{\text{P}}$ which is Eq. (60), noting that $\nu_{\text{F}} / \nu_{\text{P}} = \kappa_{\text{C}} + 1$ from Eq. (9).

On the other hand, from a thermodynamic viewpoint, the Carnot COP is $\kappa_{\text{C}} = T / (T_{\text{F}} - T)$ provided that $T_{\text{P}} \gg T_{\text{F}}$. Here the flux temperature for narrowband fluorescence is

$$T_{\text{F}} = \frac{h \nu_{\text{F}} \bar{n}_{\text{F}}}{k [(1 + \bar{n}_{\text{F}}) \ln(1 + \bar{n}_{\text{F}}) - \bar{n}_{\text{F}} \ln \bar{n}_{\text{F}}]} \quad (83)$$

from Eq. (49), where the mean photon occupation number is given by Eq. (23) as

$$\bar{n}_{\text{F}} = \frac{c^2 \dot{E}_{\text{F}}}{2\pi h \nu_{\text{F}}^3 \Delta \nu_{\text{F}} A_{\text{sample}}} \quad (84)$$

and $\dot{E}_{\text{F}} = (1 + \kappa) P_{\text{abs}} \approx P_{\text{abs}}$ according to Eq. (82). Consequently the parameters needed to calculate the ideal COP are the absorbed pump power P_{abs} , the sample's cooled temperature T and uncoated surface area A_{sample} , and the center frequency ν_{F} and bandwidth $\Delta \nu_{\text{F}}$ of the fluorescence spectrum (at temperature T). It would therefore be useful if experimentalists made it a standard practice to cite values for these five parameters in their papers.

How practical would it be to optically pump the cooler with a *nonlasing* source of light? Equation (83) gives the flux temperature T_{P} of a narrowband pump if we replace ν_{F} by ν_{P} and \bar{n}_{F} by \bar{n}_{P} where

$$\bar{n}_{\text{P}} = \frac{c^2 \dot{E}_{\text{P}}}{2h \nu_{\text{P}}^3 \Delta \nu_{\text{P}} A_{\text{pump}} \pi \sin^2 \delta_{\text{P}}} \quad (85)$$

for a pump beam of bandwidth $\Delta \nu_{\text{P}}$, divergence δ_{P} , and cross-sectional area A_{pump} . Noting from Eq. (4) that

$$\kappa_{\text{C}} = \frac{1 - \frac{T_{\text{F}}}{T_{\text{P}}}}{\frac{T_{\text{F}}}{T} - 1}, \quad (86)$$

little reduction in the Carnot COP will result as long as one maintains $T_P \gg T_F$. But $\dot{E}_F \approx \dot{E}_P$ and $v_F \approx v_P$ so that this temperature requirement becomes

$$\Delta v_P A_{\text{pump}} \sin^2 \delta_P \ll \Delta v_F A_{\text{sample}}. \quad (87)$$

Since the fluorescence and absorption bandwidths of a sample are comparable, satisfying this inequality guarantees that the pump is strongly absorbed. However, strong absorption is a necessary but not sufficient condition to obtain cooling. For example, if we simply reflected the fluorescence back to the sample (either accidentally from the walls of the sample chamber or intentionally in a misguided attempt to “recycle” the fluorescence energy) and called it “pump” light, then the left-hand side of Eq. (87) would be roughly equal to rather than much smaller than the right-hand side; that is, $T_P \approx T_F$ for that portion of the input radiation. Under ideal conditions, that would leave the COP unchanged, as we see from Eq. (86); but in reality it would *decrease* the COP according to Eq. (55), owing to background absorption, energy transfer to nonfluorescent impurities, and other heating inefficiencies.

Frey *et al.* (2000) suggest downshifting (and, implicitly, frequency narrowing and spatially collimating) the fluorescence before recycling it. More practically, one could use photovoltaics to convert some of the fluorescence into electrical energy and use that to help run the pump source. The highest possible efficiency results when the set of (uncooled) photovoltaic converters constitute a Carnot heat engine operating between the fluorescence flux temperature T_F and room temperature T_R so that

$$\varepsilon_C = \frac{T_F - T_R}{T_F} \quad (88)$$

as in Eq. (3). This efficiency is the ratio of the converted electrical power \dot{E}_R (to be recycled back perfectly to the pump power \dot{E}_P input to the optical cooler) and the collected fraction χ of the cooler’s fluorescence power \dot{E}_F , $\varepsilon_C \equiv \dot{E}_R / \chi \dot{E}_F$. The Carnot COP of the coupled refrigerator-photovoltaic system now becomes the ratio of the cooling to the net electrical work supplied,

$$\kappa_{\text{PV}} \equiv \frac{\dot{Q}}{\dot{E}_P - \dot{E}_R} = \frac{T}{T^* - T} \quad \text{where} \quad T^* \equiv \chi T_R + (1 - \chi) T_F, \quad (89)$$

since $\dot{E}_F = \dot{E}_P + \dot{Q}$ and $\dot{Q} = \dot{E}_P T / (T_F - T)$. As a check, Eq. (89) reduces to Eq. (5) if $\chi = 0$ so that there is no fluorescent recycling. On the other hand, for perfect collection ($\chi = 1$) of the fluorescence, T_F is replaced by T_R in Eq. (5) which amounts to a significant improvement in efficiency because $T_F > T_R$. In effect, we are then exhausting waste heat out of the refrigerator

system at room temperature T_R rather than at the fluorescence temperature T_F . More generally the ratio of the COP with the photovoltaic recycler to that of Eq. (5) in its absence is

$$\frac{\kappa_{PV}}{\kappa_{NPV}} = \left[1 - \chi \frac{T_F - T_R}{T_F - T} \right]^{-1}. \quad (90)$$

For example, if we use the values calculated after Eq. (66) for the current best $\text{Yb}^{3+}:\text{ZBLAN}$ cooler ($T = 208 \text{ K}$ and $T_F = 1900 \text{ K}$) assuming $T_R = 300 \text{ K}$ and say $\chi = 50\%$, then Eq. (90) predicts that one can almost double the ideal cooling performance.

In another vein, an intriguing application of fluorescent cooling is to reduce the thermal load on the medium in an optically pumped laser (Bowman 1999). Such heating results in deleterious effects such as beam defocusing by thermal lensing, depolarization due to temperature-dependent birefringence, coating delamination, and stress fractures. To reduce these effects, high-power solid-state lasers are typically water cooled. Not only does this add bulk to the entire system, it does not fully eliminate the problems, because only the surface of the laser rod or slab is being directly cooled while it is the interior that is pumped and thus there is a thermal gradient which ultimately limits the extent to which one can scale up the power. In contrast, optical cooling occurs inside the medium itself. One could start by imagining two separate systems: one pump source and set of active ions to drive the laser, and a second pump source and set of ions to run the optical cooler. Essentially this idea has been proposed by Petrushkin and Samartsev (2003) in which a KY_3F_{10} crystal is double-doped with Nd^{3+} and Yb^{3+} . Suppose the neodymium ions lase at wavelength λ_L following optical pumping at wavelength λ_P . The Stokes energy shift $hc(\lambda_P^{-1} - \lambda_L^{-1})$ is called the quantum defect and heats the crystal. However some fraction (determined by the doping concentrations) of the laser photons are absorbed in the long-wavelength tail of the ytterbium spectrum and consequently promote anti-Stokes fluorescent cooling of $hc(\lambda_F^{-1} - \lambda_L^{-1})$ per cycle. In principle, one could balance the cooling against the heating, resulting in what has been termed *athermal* laser operation. But this particular scheme for high-power scaling is limited because laser photons are being consumed by the cooling process and the laser wavelength has to be chosen to overlap the absorption band of the cooling ions and not just according to the optimal emission of the lasing ions.

A clever alternative dispenses with the need for a separate optical cooling system and uses a single pumped set of active ions which both lase by Stokes-shifted stimulated emission and fluoresce by anti-Stokes-shifted spontaneous emission. This is done by choosing a pump photon frequency which is intermediate between the mean fluorescence frequency and the laser output frequency (selected by appropriate design of the feedback cavity mirrors), $\nu_L < \nu_P < \nu_F$. Using a biaxial host such as $\text{KGd}(\text{WO}_4)_2$, one can choose the pump wavelength and polarization to coincide with an absorption peak and independently choose the laser wavelength and

polarization to match an emission peak. Athermal operation occurs when two balance conditions are met in each volume element of the laser medium: both the rates and the powers for absorption and (spontaneous plus stimulated) emission must be equal, using equations similar to those of Eqs. (67) and (71). Such a laser is said to be *radiation balanced*. A combined optical and thermodynamic analysis of a single-pass radiation-balanced $\text{Yb}^{3+}:\text{KGd}(\text{WO}_4)_2$ amplifier has been undertaken by Mungan (2003) and its Carnot efficiency for the ratio of the output laser power to the input pump power is $\varepsilon_C \equiv \dot{E}_L / \dot{E}_P = 1 - T_F / T_P$, since ideally the laser is a heat engine operating between the pump and fluorescence flux temperatures. An oscillator model has been discussed by Li *et al.* (2004).

Consider the thermal load on a continuous-wave (CW) laser medium in the ideal case where there is no reabsorption, nonradiative relaxation, or background absorption. At steady state, the rate of optical pumping (transitions per second) up to the excited state must balance the relaxation rate back down to the ground state by lasing and fluorescence,

$$\dot{N}_P = \dot{N}_L + \dot{N}_F \quad \Rightarrow \quad \frac{\dot{E}_F}{h\nu_F} = \frac{\dot{E}_P}{h\nu_P} - \frac{\dot{E}_L}{h\nu_L}. \quad (91)$$

Cooling of the medium results from the difference between the radiative fluxes out of and into it,

$$\dot{Q} = \dot{E}_L + \dot{E}_F - \dot{E}_P. \quad (92)$$

Defining the cooling COP to be $\kappa_{\text{cool}} \equiv \dot{Q} / \dot{E}_P$ and the optical-to-optical lasing efficiency as $\varepsilon_{\text{lase}} \equiv \dot{E}_L / \dot{E}_P$, then one can substitute Eq. (91) into (92) to obtain

$$\kappa_{\text{cool}} = \kappa_F(1 - \varepsilon_{\text{lase}}) - \kappa_L \varepsilon_{\text{lase}} \lambda_L / \lambda_F \quad (93)$$

where the the cooling COP in the absence of lasing ($\varepsilon_{\text{lase}} = 0$) is $\kappa_F \equiv (\lambda_P - \lambda_F) / \lambda_F$ as in Eq. (9), and the lasing fractional quantum defect is $\kappa_L \equiv (h\nu_P - h\nu_L) / h\nu_P = (\lambda_L - \lambda_P) / \lambda_L$. The first expression on the right-hand side of Eq. (93) thus represents the relative cooling due to the fluorescence, while the second term is the relative heating due to the lasing. (Note in particular that $\kappa_{\text{cool}} = -\kappa_L$ if $\dot{E}_F = 0$.) For radiation balancing, $\kappa_{\text{cool}} = 0$ and Eq. (93) then implies that the optical efficiency is

$$\varepsilon_{\text{lase}} = \frac{\lambda_P - \lambda_F}{\lambda_L - \lambda_F}. \quad (94)$$

The choice of wavelengths consistent with the frequencies discussed above, $\lambda_L > \lambda_P > \lambda_F$, implies that $0 < \varepsilon_{\text{lase}} < 1$. Also note for this athermal case that the fraction of the pump power that is converted into fluorescence is $\dot{E}_F / \dot{E}_P = 1 - \varepsilon_{\text{lase}}$.

Even if perfect radiation balancing is not attained, one can reduce the heat load on the medium. For example Bowman *et al.* (2005) have constructed a quasi-CW thin-disk $\text{KGd}(\text{WO}_4)_2$

laser doped with 3 at% Yb^{3+} and edge-pumped with 90 diode laser bars (corresponding to an incident power of 2.25 kW) at $\lambda_p = 993 \text{ nm}$. The highest output power $\dot{E}_L = 0.49 \text{ kW}$ at $\lambda_L = 1047 \text{ nm}$ resulted when $\dot{E}_p = 1.10 \text{ kW}$ of the pump power was absorbed, corresponding to an optical efficiency of $\varepsilon_{\text{lase}} = 45\%$. Using a powdered sample to minimize radiation trapping, the mean fluorescence wavelength was measured to be $\lambda_F = 997 \text{ nm}$. (Therefore the pump wavelength, although a good match to an ytterbium absorption peak, was not long enough to produce athermal operation. It was limited by the available InGaAs laser diodes.) Consequently one computes the nonlasing cooling COP to be $\kappa_F = -0.4\%$ and the lasing quantum defect to be $\kappa_L = +5.2\%$. Equation (93) thus predicts $-\kappa_{\text{cool}} = 2.7\%$, whereas the measured thermal loading was found to be 3.2%. The discrepancy results from the fact that the fluorescence wavelength is redshifted by reabsorption to $\lambda_F^* = \lambda_F / \eta_{\text{ext}}$ from Eq. (61) where the external fluorescence quantum efficiency is given by Eq. (81). Estimating the fluorescence lineshape function $g(\lambda)$ to be divided by $1 + \alpha_{\text{res}}(\lambda)L$ due to reabsorption, where α_{res} is the ytterbium absorption coefficient and L is the effective length of the laser crystal (approximately double its 8-mm diameter) treated as an optical cavity, the trapped fluorescence wavelength is calculated to be $\lambda_F^* = 1011 \text{ nm}$, which accounts for the extra thermal loading.

In principle, average athermal operation is possible not just for CW but also for pulsed lasers such as kilohertz Q -switched ytterbium-doped systems (Wang *et al.* 2007). The idea is that net fluorescent cooling during the time that the Q switch is off can compensate for a large transient thermal load when it is on, assuming that the pump source consists of continuous diode lasers. Another new concept (Vermeulen *et al.* 2007) for mitigating the quantum-defect heating of a laser by optical cooling takes advantage of coherent anti-Stokes Raman scattering (CARS), in which a pump and a Stokes-shifted photon are converted into a pump and an anti-Stokes photon, with the associated annihilation of two phonons. As an example, a phase-matched CW silicon waveguide laser has been modeled that emits 0.69 W at a Stokes wavelength of 3.14 μm and 0.43 W at an anti-Stokes wavelength of 2.37 μm when pumped by a 5 W fiber laser at 2.7 μm . By having increased the ratio of anti-Stokes to Stokes photons, the simulations indicate that the thermal load is reduced by 35% compared to the heating in the absence of CARS. An alternative to CARS in a single medium such as silicon is coherent four-wave mixing in a doped material such as $\text{Yb}^{3+}:\text{YAG}$ (Muys 2008). Lasing occurs by Stokes shifting one pump photon at a dopant site, while cooling occurs by anti-Stokes shifting a second pump photon at a host site.

It will be interesting to see whether the first practical application of solid-state optical cooling outside of the laboratory will be to a refrigerator or to a laser. Time will tell.

References

- A. Arakengy (1957). *Liouville's theorem and the intensity of beams*. Am. J. Phys. **25**, 519–525.
- S.R. Bowman (1999). *Lasers without internal heat generation*. IEEE J. Quantum Electron. **35**, 115–122.
- S.R. Bowman and C.E. Mungan (2000). *New materials for optical cooling*. Appl. Phys. B **71**, 807–811.
- S.R. Bowman, S.P. O'Connor, and S. Biswal (2005). *Ytterbium laser with reduced thermal loading*. IEEE J. Quantum Electron. **41**, 1510–1517.
- A.H. Carter (2001). Classical and Statistical Thermodynamics (Prentice-Hall, Upper Saddle River), Chap. 20.
- Y. Chen, A. Rapaport, T.-Y. Chung, B. Chen, and M. Bass (2003). *Fluorescence losses from Yb:YAG slab lasers*. Appl. Opt. **42**, 7157–7162.
- J.L. Clark, P.F. Miller, and G. Rumbles (1998). *Red edge photophysics of ethanolic rhodamine 101 and the observation of laser cooling in the condensed phase*. J. Phys. Chem. A **102**, 4428–4437.
- N. Djeu and W.T. Whitney (1981). *Laser cooling by spontaneous anti-Stokes scattering*. Phys. Rev. Lett. **46**, 236–239.
- G.C. Dousmanis, C.W. Mueller, H. Nelson, and K.G. Petzinger (1964). *Evidence of refrigerating action by means of photon emission in semiconductor diodes*. Phys. Rev. **133**, A316–A318.
- B.C. Edwards, J.E. Anderson, R.I. Epstein, G.L. Mills, and A.J. Mord (1999). *Demonstration of a solid-state optical cooler: An approach to cryogenic refrigeration*. J. Appl. Phys. **86**, 6489–6493.
- R.I. Epstein, M.I. Buchwald, B.C. Edwards, T.R. Gosnell, and C.E. Mungan (1995). *Observation of laser-induced fluorescent cooling of a solid*. Nature (London) **377**, 500–503.
- C. Essex, D.C. Kennedy, and R.S. Berry (2003). *How hot is radiation?* Am. J. Phys. **71**, 969–978.
- G.R. Fowles (1989). Introduction to Modern Optics, 2nd ed. (Dover, New York), Chap. 7.
- R. Frey, F. Micheron, and J.P. Pocholle (2000). *Comparison of Peltier and anti-Stokes optical coolings*. J. Appl. Phys. **87**, 4489–4498.
- P. Gerthsen and E. Kauer (1965). *The luminescence diode acting as a heat pump*. Phys. Lett. **17**, 255–256.
- J.E. Geusic, E.O. Schulz-DuBois, and H.E.D. Scovil (1967). *Quantum equivalent of the Carnot cycle*. Phys. Rev. **156**, 343–351.
- B. Heeg, P.A. DeBarber, and G. Rumbles (2005). *Influence of fluorescence reabsorption and trapping on solid-state optical cooling*. Appl. Opt. **44**, 3117–3124.

- C.W. Hoyt, M.P. Hasselbeck, M. Sheik-Bahae, R.I. Epstein, S. Greenfield, J. Thiede, J. Distel, and J. Valencia (2003a). *Advances in laser cooling of thulium-doped glass*. J. Opt. Soc. Am. B **20**, 1066–1074.
- C.W. Hoyt, W. Patterson, M.P. Hasselbeck, M. Sheik-Bahae, R.I. Epstein, J. Thiede, and D. Seletskiy (2003b). *Laser cooling thulium-doped glass by 24 K from room temperature*. IEEE Conf. Proc. QELS Postconference Digest, pp. 790–795.
- O. Kafri and R.D. Levine (1974). *Thermodynamics of adiabatic laser processes: Optical heaters and refrigerators*. Opt. Commun. **12**, 118–122.
- T. Kushida and J.E. Geusic (1968). *Optical refrigeration in Nd-doped yttrium aluminum garnet*. Phys. Rev. Lett. **21**, 1172–1175.
- G. Lamouche, P. Lavallard, R. Suris, and R. Grousseau (1998). *Low temperature laser cooling with a rare-earth doped glass*. J. Appl. Phys. **84**, 509–516.
- L. Landau (1946). *On the thermodynamics of photoluminescence*. J. Phys. (Moscow) **10**, 503–506.
- P.T. Landsberg and D.A. Evans (1968). *Thermodynamic limits for some light-producing devices*. Phys. Rev. **166**, 242–246.
- P.T. Landsberg and G. Tonge (1980). *Thermodynamic energy conversion efficiencies*. J. Appl. Phys. **51**, R1–R20.
- G. Lei, J.E. Anderson, M.I. Buchwald, B.C. Edwards, R.I. Epstein, M.T. Murtagh, and G.H. Sigel, Jr. (1998). *Spectroscopic evaluation of Yb³⁺-doped glasses for optical refrigeration*. IEEE J. Quantum Electron. **34**, 1839–1845.
- K. Lehovec, C.A. Accardo, and E. Jamgochian (1953). *Light emission produced by current injected into a green silicon-carbide crystal*. Phys. Rev. **89**, 20–25.
- C. Li, Q. Liu, M. Gong, G. Chen, and P. Yan (2004). *Modeling of radiation-balanced continuous-wave laser oscillators*. J. Opt. Soc. Am. B **21**, 539–542.
- G. Liakhov, S. Paoloni, and M. Bertolotti (2004). *Observations of laser cooling by resonant energy transfer in CO₂-N₂ mixtures*. J. Appl. Phys. **96**, 4219–4224.
- R. Loudon (1990). The Quantum Theory of Light, 2nd ed. (Clarendon, Oxford), Chap. 1.
- C.E. Mungan and T.R. Gosnell (1999). *Laser cooling of solids* in Advances in Atomic, Molecular, and Optical Physics, edited by B. Bederson and H. Walther (Academic Press, San Diego), Vol. 40, pp. 161–228.
- C.E. Mungan (2003). *Thermodynamics of radiation-balanced lasing*. J. Opt. Soc. Am. B **20**, 1075–1082.
- C.E. Mungan (2005). *Radiation thermodynamics with applications to lasing and fluorescent cooling*. Am. J. Phys. **73**, 315–322.

- C.E. Mungan, M.I. Buchwald, and G.L. Mills (2007). *All-solid-state optical coolers: History, status, and potential* in Cryocoolers 14, edited by S.D. Miller and R.G. Ross, Jr. (ICC Press, Boulder), pp. 539–548.
- P. Muys (2008). *Stimulated radiative laser cooling*. Laser Physics **18**, 430–433.
- W. Nakwaski (1982). *Optical refrigeration in light-emitting diodes*. Electron Tech. **13**, 61–76.
- F.E. Nicodemus (1965). *Directional reflectance and emissivity of an opaque surface*. Appl. Opt. **4**, 767–773.
- S.V. Petrushkin and V.V. Samartsev (2003). *Laser cooling of active media in solid-state lasers*. Laser Physics **13**, 1290–1296.
- P. Pringsheim (1929). *Zwei Bemerkungen über den Unterschied von Lumineszenz- und Temperaturstrahlung*. Z. Physik **57**, 739–746.
- P. Pringsheim (1946). *Some remarks concerning the difference between luminescence and temperature radiation: Anti-Stokes fluorescence*. J. Phys. (Moscow) **10**, 495–498.
- R.T. Ross (1966). *Thermodynamic limitations on the conversion of radiant energy into work*. J. Chem. Phys. **45**, 1–7.
- X.L. Ruan, S.C. Rand, and M. Kaviani (2007). *Entropy and efficiency in laser cooling of solids*. Phys. Rev. B **75**, 214304:1–9.
- M. Sheik-Bahae and R.I. Epstein (2007). *Optical refrigeration*. Nature Photonics **1**, 693–699.
- J. Tauc (1957). *The share of thermal energy taken from the surroundings in the electro-luminescent energy radiated from a p–n junction*. Czech. J. Phys. **7**, 275–276.
- J. Thiede, J. Distel, S.R. Greenfield, and R.I. Epstein (2005). *Cooling to 208 K by optical refrigeration*. Appl. Phys. Lett. **86**, 154107:1–3.
- D.A. Van Baak (1995). *Just how bright is a laser?* Phys. Teach. **33**, 497–499.
- S. Vavilov (1945). *Some remarks on the Stokes law*. J. Phys. (Moscow) **9**, 68–72.
- S. Vavilov (1946). *Photoluminescence and thermodynamics*. J. Phys. (Moscow) **10**, 499–502.
- N. Vermeulen, C. Debaes, P. Muys, and H. Thienpont (2007). *Mitigating heat dissipation in Raman lasers using coherent anti-Stokes Raman scattering*. Phys. Rev. Lett. **99**, 093903:1–4.
- J.-B. Wang, S.R. Johnson, D. Ding, S.-Q. Yu, and Y.-H. Zhang (2006). *Influence of photon recycling on semiconductor luminescence refrigeration*. J. Appl. Phys. **100**, 043502:1–5.
- X. Wang, D. Cao, M. Zhou, and J. Tan (2007). *Q-switched lasers with optical cooling*. J. Opt. Soc. Am. B **24**, 2213–2217.
- M.A. Weinstein (1960). *Thermodynamic limitation on the conversion of heat into light*. J. Opt. Soc. Am. **50**, 597–602.
- D.J. Wineland and W.M. Itano (1987). *Laser cooling*. Phys. Today **40** (6), 34–40.

Figure 1. Simplified characterization of the energy input to and output from an optical cooler. Thermal energy is withdrawn from the cooling medium itself, as well as from any external load attached to it. The refrigerator is driven by a low-entropy source, such as a laser resonant with the low-energy wing of an absorption band of the cooling material. Finally, the medium relaxes radiatively and the output fluorescence carries energy away to some external heat sink.

Figure 2. Relevant energy levels of a gas of neutral sodium atoms. First the D_1 transition is pumped at 589.6 nm using a spectrally filtered sodium lamp. Then the two upper P levels thermalize with each other, so that they end up with nearly equal population densities (according to the Boltzmann distribution at room temperature). Finally one gets emission on both the D_1 and D_2 lines, with the latter having a slightly shorter photon wavelength of 589.0 nm and thus a slightly larger photon energy.

Figure 3. A heat engine and a refrigerator coupled in tandem between three thermal baths as a model for an optical cooler. In one excitation-relaxation cycle, energy E_{in} is absorbed from the pump source, heat Q is withdrawn from the cooling sample (and its load), and net energy $E_{\text{out}} \equiv E_{\text{out,engine}} + E_{\text{out,fridge}}$ is exhausted in the form of fluorescence. All of the work W output from the engine is used to drive the fridge.

Figure 4. Coupling of a three-level system to a set of thermal reservoirs that maintain Boltzmann population ratios at the appropriate temperatures and transition frequencies. In order to maximize the cooling efficiency, spontaneous emission between levels 2 and 1 has been neglected.

Figure 5. Portion of the radiation emitted from surface area dA of the sample into solid angle $d\Omega$. The polar angle θ is measured relative to the surface normal direction defining the z axis, while the azimuthal angle ϕ is measured counter-clockwise from the x axis aligned along any convenient direction tangential to the sample surface.

Figure 6. Three examples of plots of some spectral quantity F_λ versus wavelength λ . Each is characterized by three values: λ_0 denoted by the solid vertical line and equal to the centroid of the spectrum, F_0 indicated by the height of the dashed rectangle and equal to the peak value of F_λ , and $\Delta\lambda$ represented by the width of the dashed rectangle and chosen so that the areas under the spectrum and under the dashed rectangle are equal. (a) A single Gaussian peak. (b) A series of three spikes that might represent emission from a multimode diode laser. (c) Sum of a pair of Lorentzians composing a peak with a long-wavelength shoulder.

Figure 7. Comparison of the spectral radiance of a 2000 K blackbody and of the ytterbium-doped heavy-metal-fluoride fluorescence (approximated as a Gaussian peaking at 995 nm with a 35 nm bandwidth) corresponding to a hemispherical emittance of $\dot{E}_F / A_{\text{sample}} = 0.94 \text{ W/cm}^2$.

Figure 8. Distinction between unidirectional light emanating from differential surface area dA_1 and divergent light from area dA_2 . Although the radiation in region 1 is overall not a plane wave, it could represent a portion of a single spherical optical mode emitted by a point source located at the center of curvature, whereas the light issuing from a fixed (x, y) location in region 2 is distributed over a range of angles θ and ϕ (and hence over many modes). The curve representing the overall surface A could be the actual boundary of a sample emitting radiation or it could simply be an arbitrary surface in space that the radiation happens to be crossing.

Figure 9. Average brightness \bar{T}_b and flux T_f temperatures for narrowband infrared light peaking at $\lambda_0 = 1 \mu\text{m}$ as a function of its mean spectral radiance \bar{L}_λ . The abscissa spans values ranging from low-power lamps up to high-brightness lasers. A radiation temperature is thus a useful, intensive figure of merit for evaluating the quality of an optical source at a given center wavelength; it characterizes the width of the distribution of energy among the optical modes.

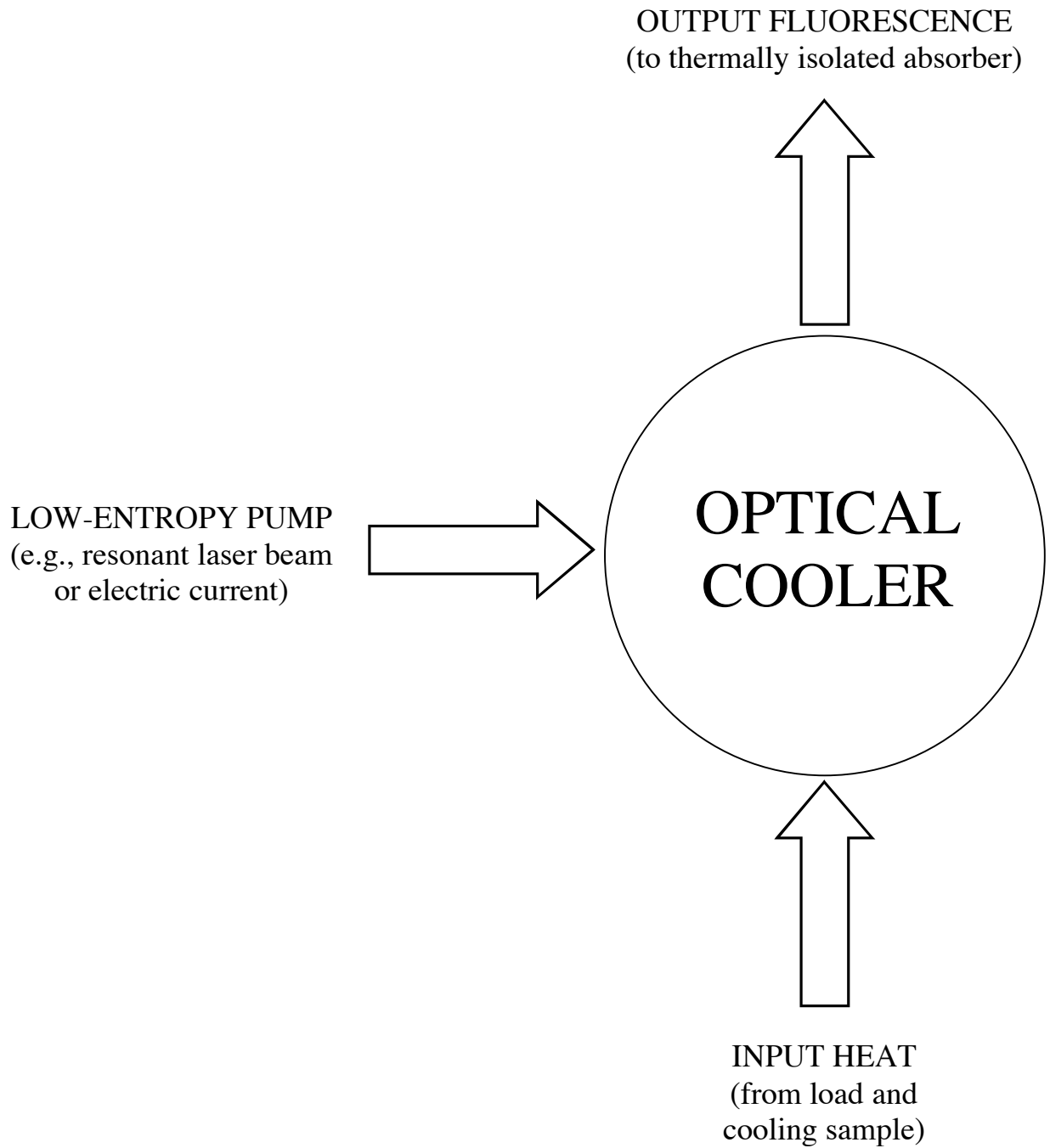
Figure 10. Flow diagram analogous to Fig. 1 for the rate at which energy and entropy are transported into and out of a fluorescent refrigerator or, in the case of entropy S_G , is spontaneously generated during the cooling process. (Note that this latter entropy does not accumulate in the system in steady state because the entropy of the cooling sample, which is a function of state, must return to its initial value at the completion of each cycle. More entropy leaves than enters the system, as many of the processes occurring within the sample are irreversible.) To correspond to Fig. 3, identify E_P with E_{in} and E_F with E_{out} .

Figure 11. Cylindrical cross-section of an optical cooler operating at temperature T . The blackened walls of the vacuum chamber are maintained at ambient temperature T_A using an external coolant. The pump radiation is reflected between mirrors (not shown) parallel to the flat faces of the sample; one of these high reflectors could have a small input hole to admit fiber-coupled pump light (Edwards 1999). The heat shield is assumed to have negligible emissivity (and thus absorptivity), reflecting all thermal radiation at long wavelengths and transmitting all fluorescence at short wavelengths. The sample reflects or transmits some of the incident thermal flux with occupation number n_T ; it absorbs and then re-emits the remaining portion.

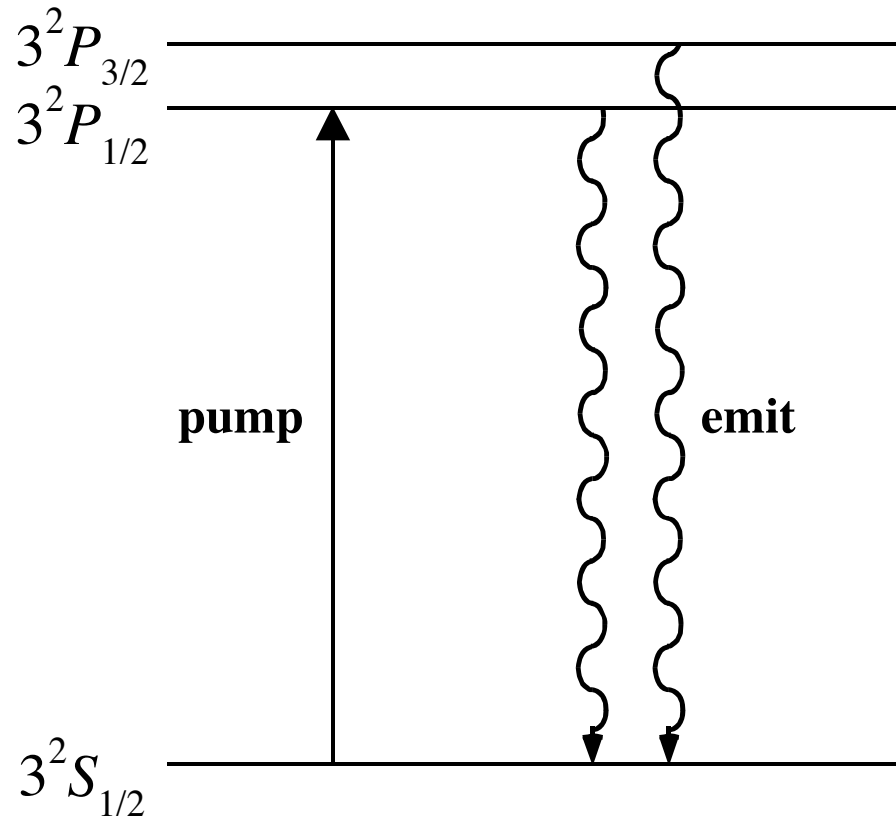
Figure 12. Plots of κ_C and of \dot{Q}/T (in the Carnot limit) for pump powers \dot{E}_P ranging from 1 W to 1 MW. As in Sec. III, the cooling sample is assumed to have a surface area of $A_{\text{sample}} = 13.5\pi \text{ cm}^2$ and the fluorescence spectrum is that of $\text{Yb}^{3+}:\text{ZBLAN}$ at room temperature, peaking at $\lambda_F = 995 \text{ nm}$ with a bandwidth of $\Delta\lambda_F = 35 \text{ nm}$. The Carnot COP is computed at $T = 300 \text{ K}$ assuming $T_P \gg T_F$.

Figure 13. Ratio of the cooling coefficient of performance κ to its unsaturated value $\kappa_{\text{unsat}} \equiv \eta_{\text{ext}} \lambda_P / \lambda_F - 1$ plotted against pump intensity I varying over a range from a thousandth to a thousand times the saturation intensity I_{sat} . Note in particular that the COP is halved when one drives the cooler at I_{sat} , because at saturation half of the emissions are stimulated rather than spontaneous and so do not contribute to cooling.

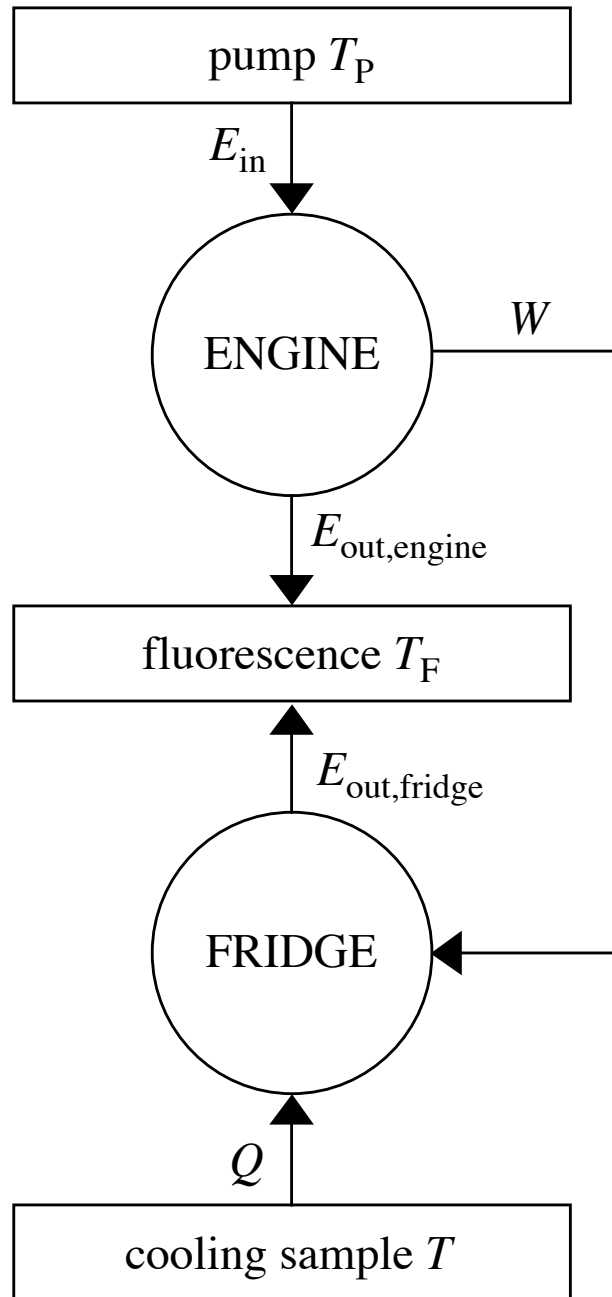
Figure 14. Plot of the COP κ versus the pump wavelength λ_P for 1 wt% $\text{Yb}^{3+}:\text{ZBLAN}$ at room temperature assuming a mean fluorescence wavelength of $\lambda_F = 995 \text{ nm}$, an external fluorescence quantum efficiency of $\eta_{\text{ext}} = 99\%$, and a background absorption coefficient of $\alpha_{\text{back}} = 10^{-4} \text{ cm}^{-1}$. The pump intensity is presumed to be much weaker than the saturation intensity, $I \ll I_{\text{sat}}$, at all wavelengths longer than 990 nm.



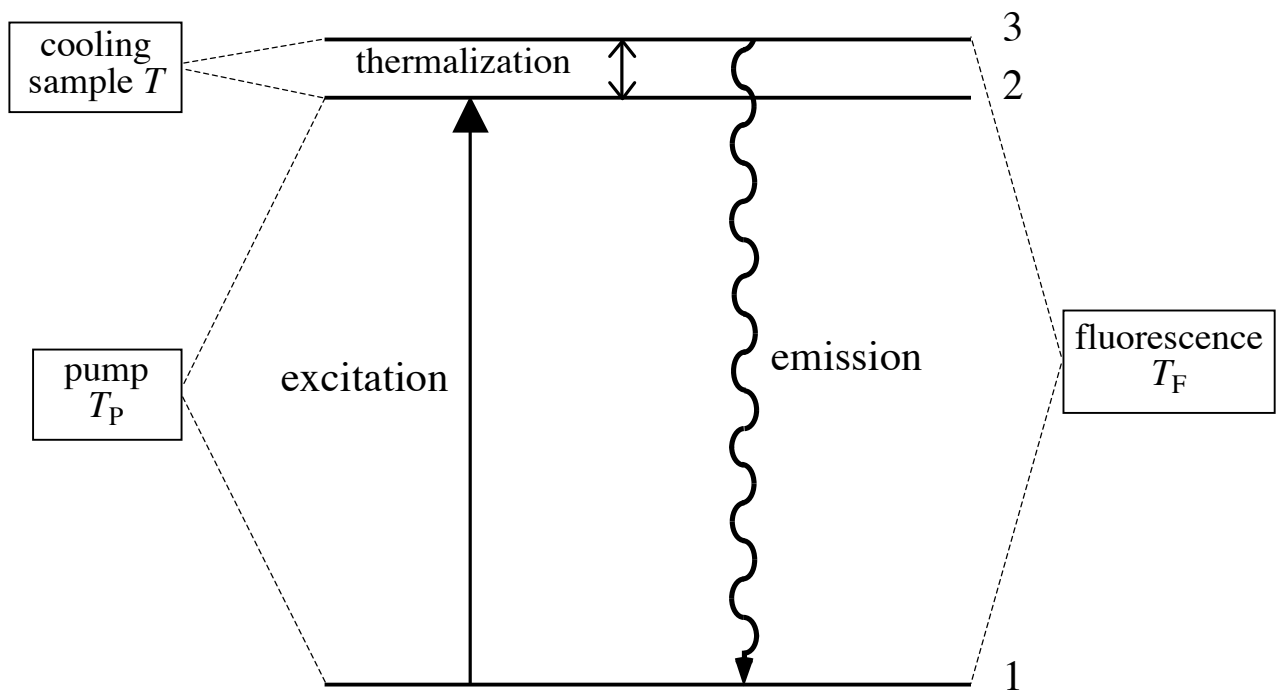
Mungan Fig. 1



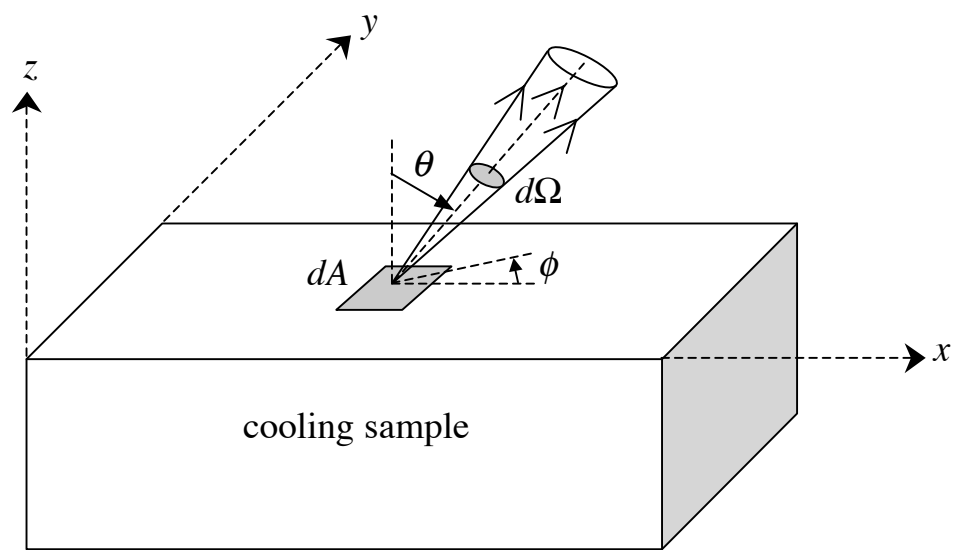
Mungan Fig. 2



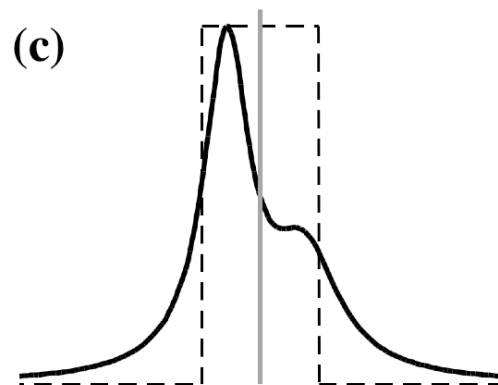
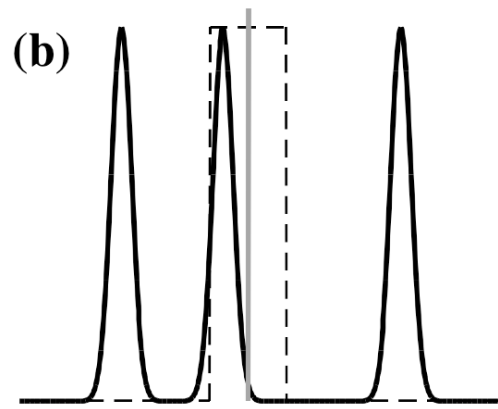
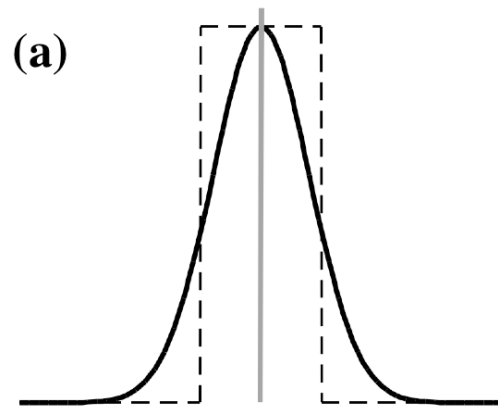
Mungan Fig. 3



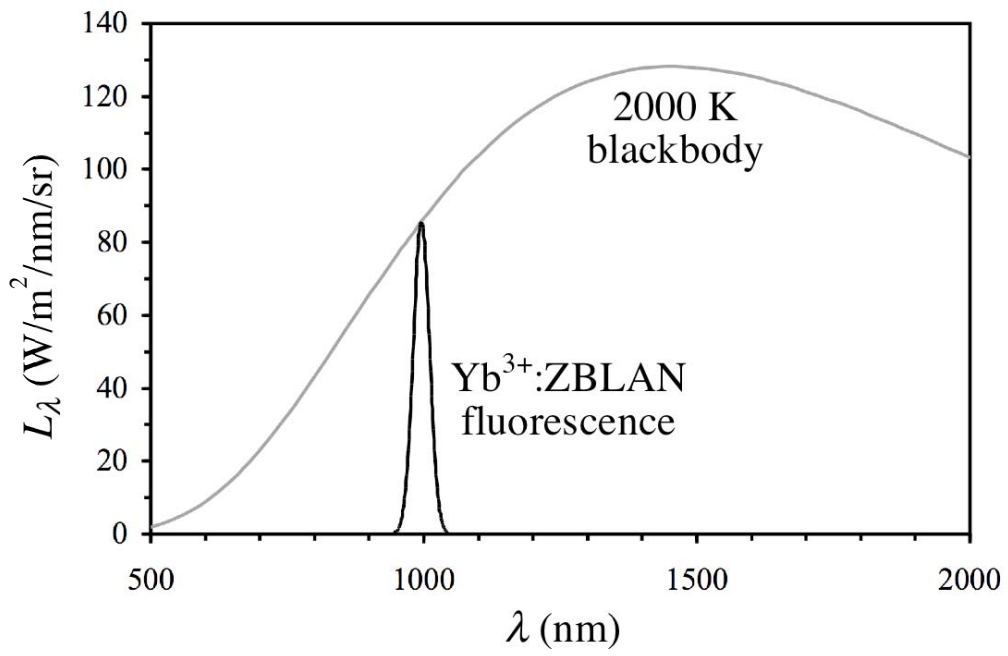
Mungan Fig. 4



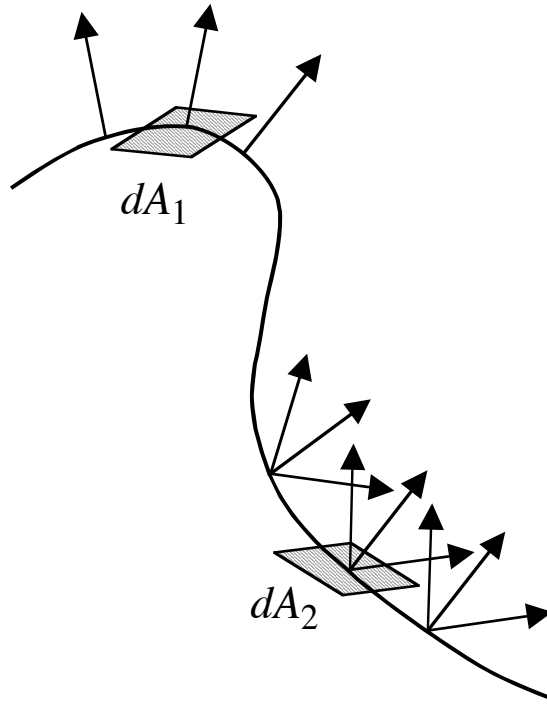
Mungan Fig. 5



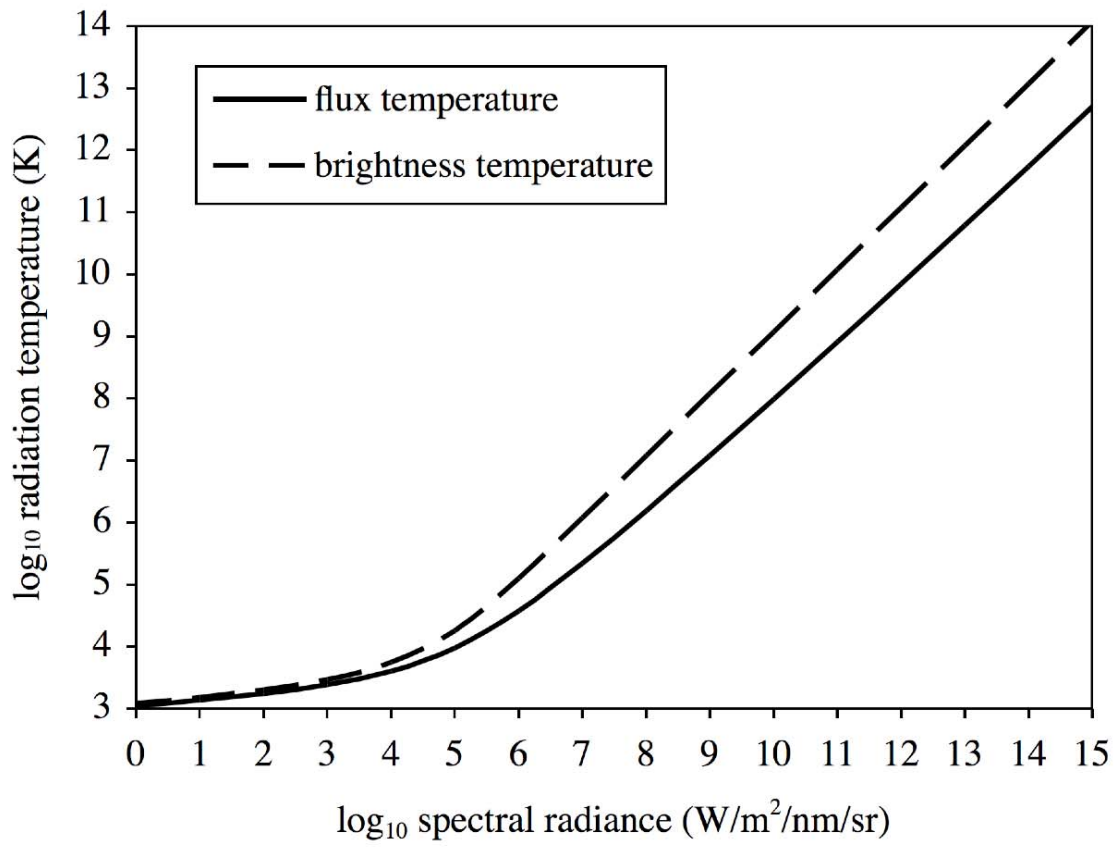
Mungan Fig. 6



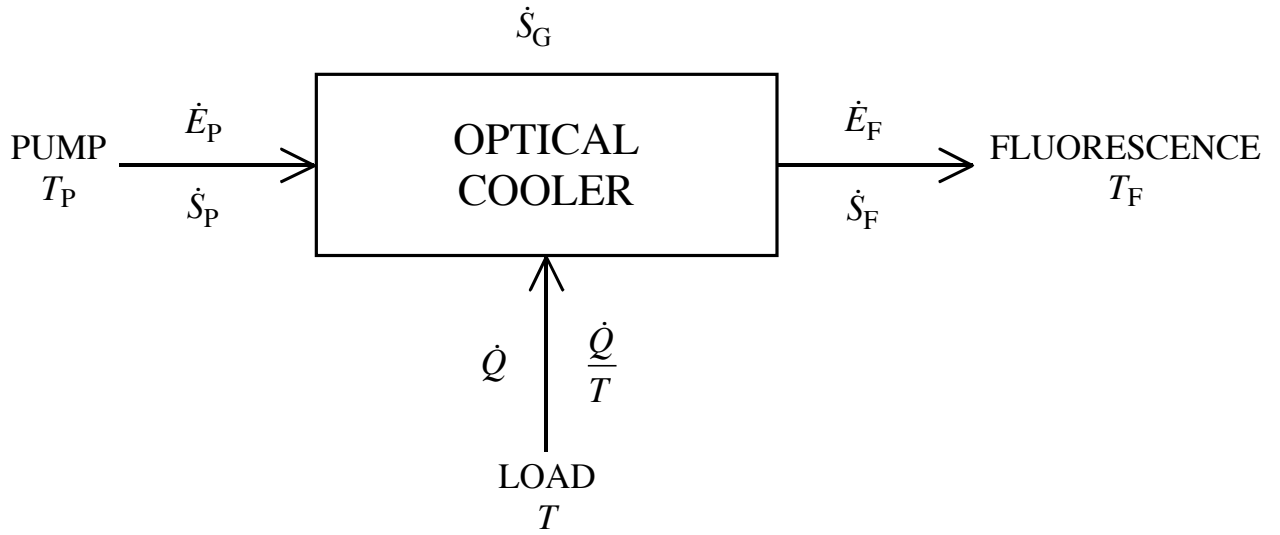
Mungan Fig. 7



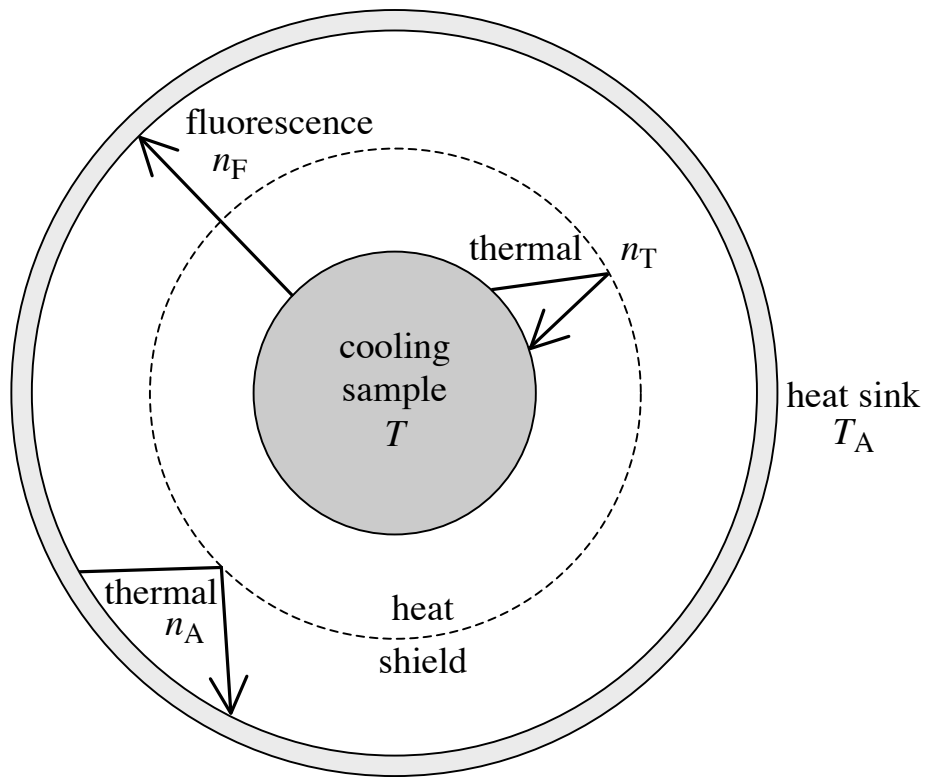
Mungan Fig. 8



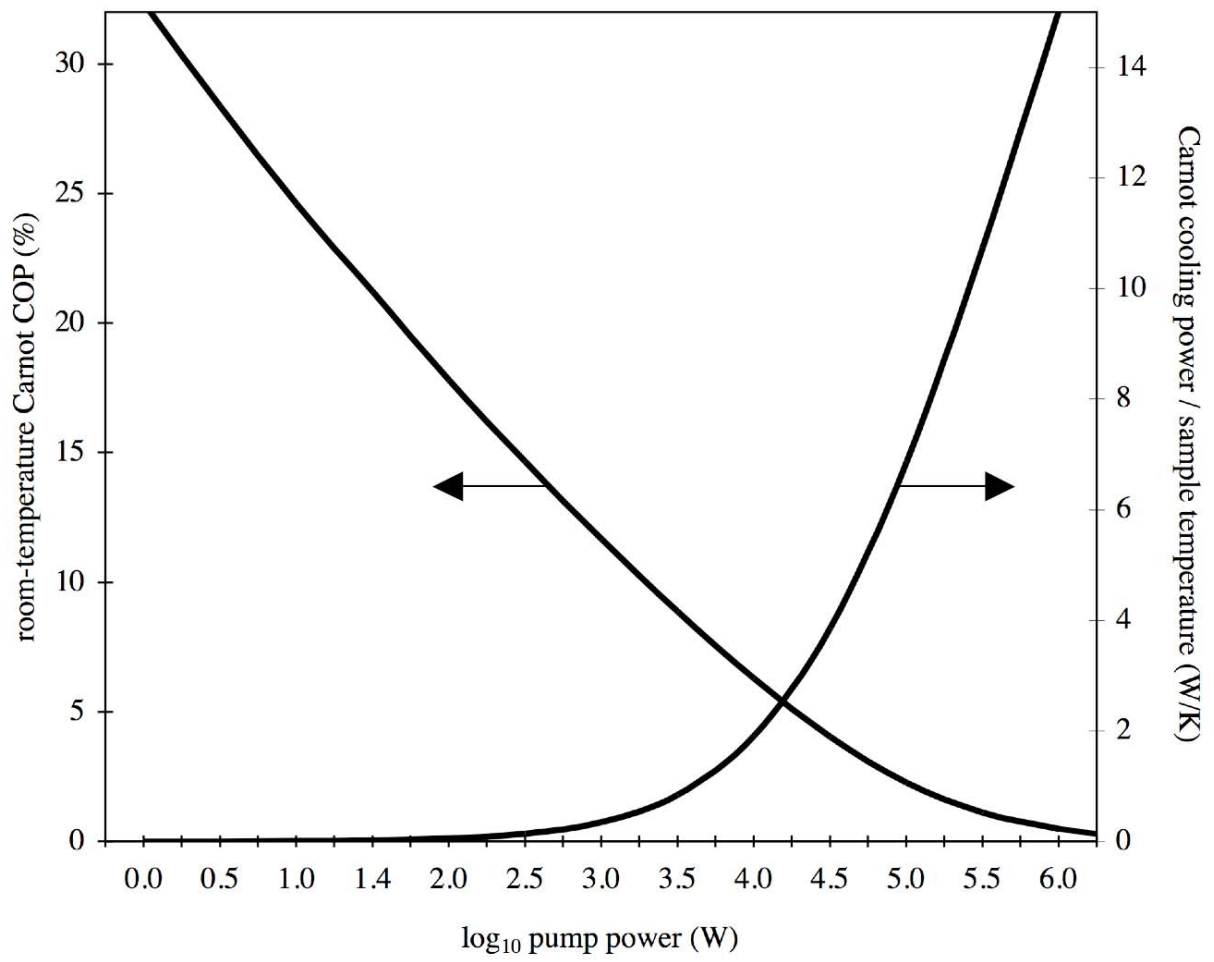
Mungan Fig. 9



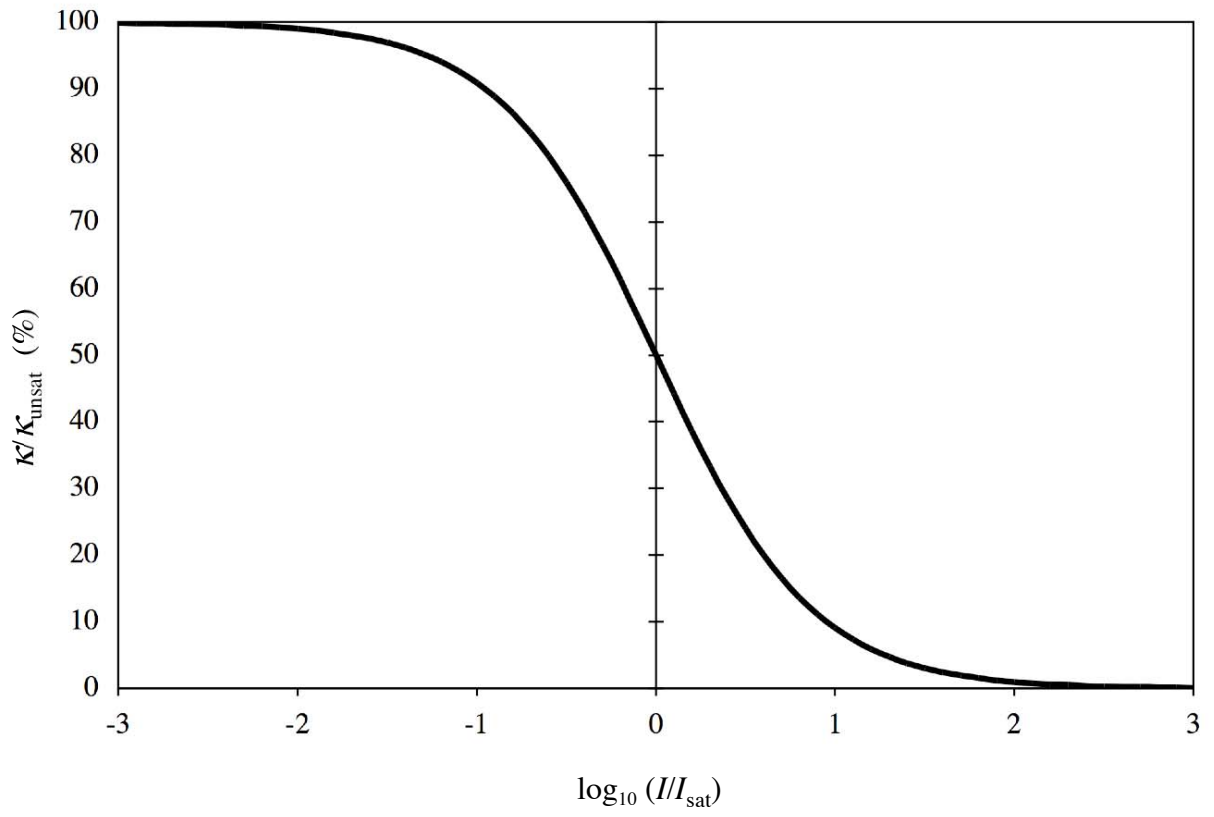
Mungan Fig. 10



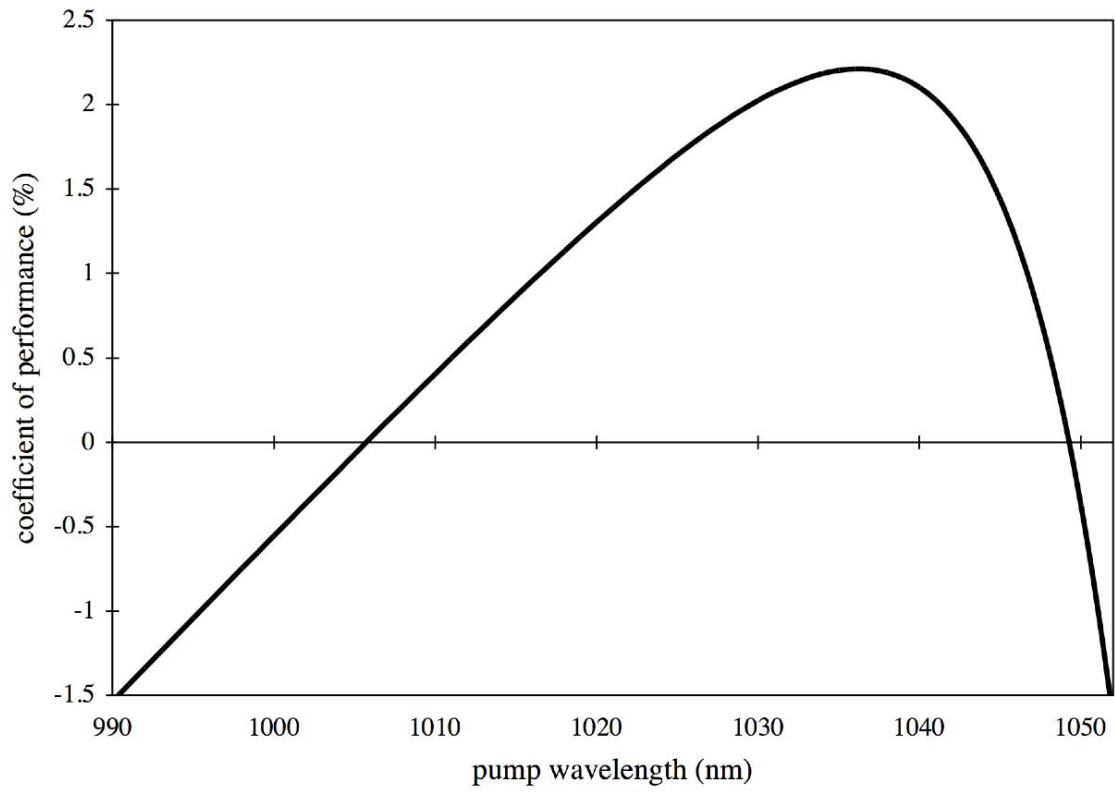
Mungan Fig. 11



Mungan Fig. 12



Mungan Fig. 13



Mungan Fig. 14